FA9550-20-1-0135
W911NF-2210130

Impact of Stress and Strain on Optical Spectra of Semiconductors

Stefan Zollner

Department of Physics
New Mexico State University
Las Cruces, NM, USA

Email: zollner@nmsu.edu. WWW: http://femto.nmsu.edu.
Ask me about MS/Ph.D. student positions at NMSU..

Biography

Regensburg/Stuttgart
Germany

Motorola (Mesa, Tempe)
Arizona, 1997-2005

Freescale, IBM
New York, 91-92;07-10

Las Cruces, NM
Since 2010

Motorola, Freescale
Texas, 2005-2007

Where is Las Cruces, NM ???

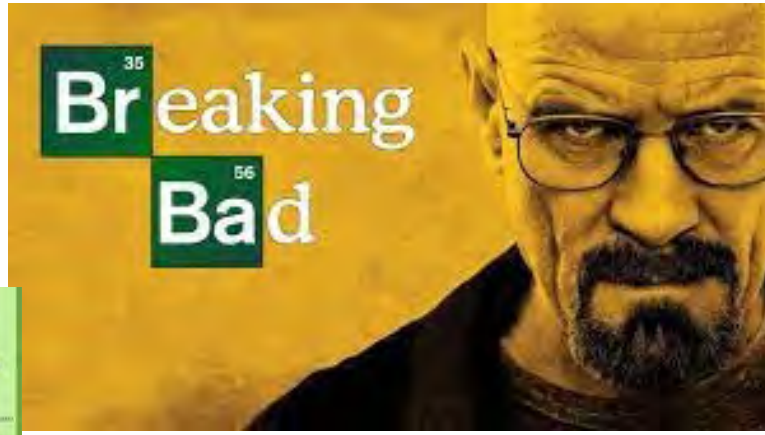

White Sands NP

Finally in Grenoble

STM fab in Crolles

Dès 1972, une collaboration est engagée entre le SNCI et le **Max-Plank-Institut für Festkörperforschung (MPI-FKF)** de Stuttgart (avec Dransfeld). La puissance est portée à 10 MW en 1974, ce qui permet d'atteindre en 1982 des champs de 25T dans un diamètre de 50 mm, avec les premières polyhélices construites par Hans Schneider-Muntau. C'est dans les champs intenses de Grenoble que **Klaus von Klitzing** découvre l'effet Hall quantique entier dans la nuit du 4 au 5 février 1980, qui lui vaut le prix Nobel de physique en 1985.

Dr. Maria Spies
Universite Grenoble Alpes

Now a physics postdoc in Pisa.

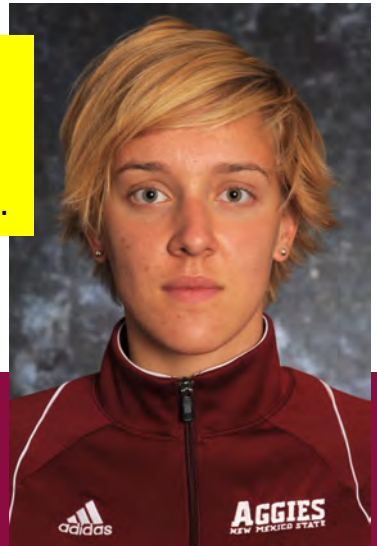

soitec

Outline: tutorial on stress and strain

- Hooke's Law
- Stress and strain tensors
- Elasticity and compliance tensors
- Examples of stress along one, two, and three directions
- Strain measurements using high-resolution x-ray diffraction
- Impact of strain on phonon energies (Raman spectra)
- Impact of strain on band energies with CMOS applications
- Impact of strain on optical spectra of semiconductors
- Example: Pseudomorphic Ge-Sn alloy layer on GaAs

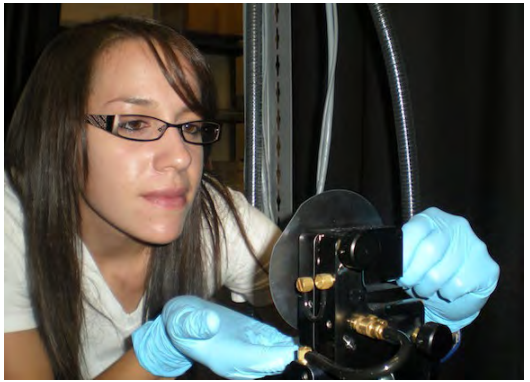

Hooke's Law

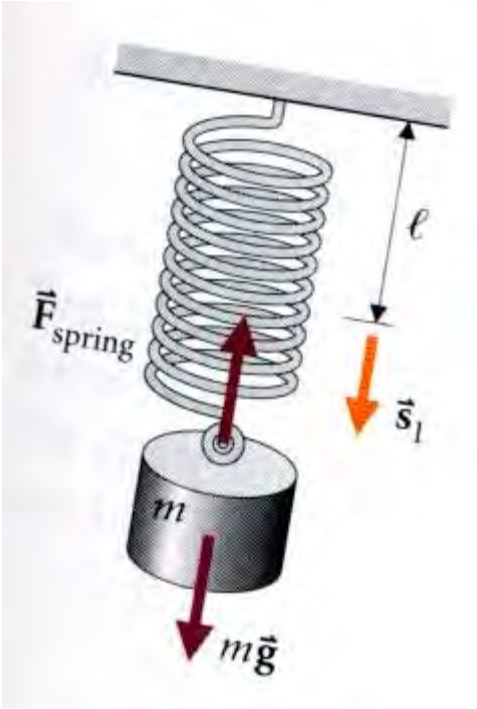

$$F = mg = ks_l$$

In one dimension, the **stress** is the force (measured in N).
The **strain** is the relative length change (dimensionless).
k is the **spring constant** (elasticity constant).

Let's rewrite this:

r	Length of unstretched spring (m)
r'	Length of stretched spring (m)
u=r'-r	Displacement of spring (m)
ε=u/r	Strain (relative displacement), dimensionless
c=kr	Elasticity constant (N)
F=cε	**Hooke's Law in one dimension**

$$F = c\varepsilon$$

Stress tensor

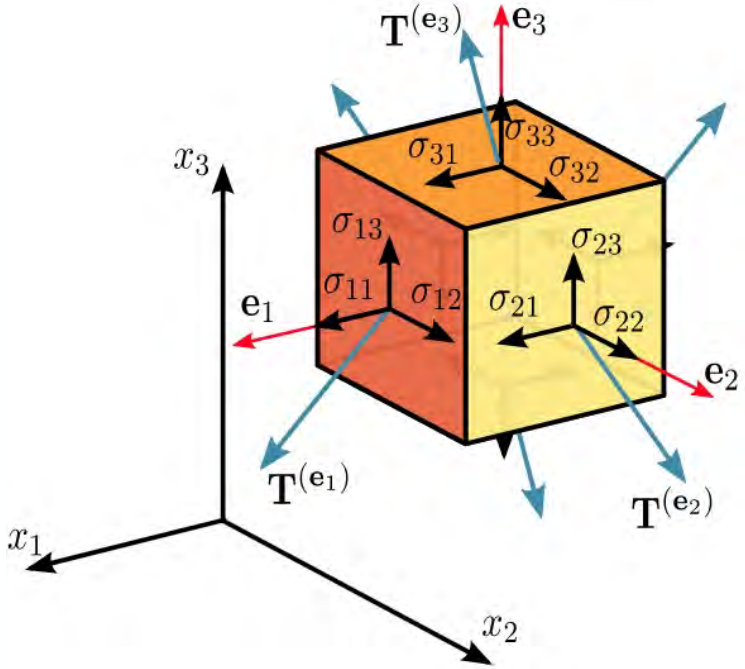

Stress defined as **force per unit area**.
Measured in units of MPa or GPa.

Sum of all forces (net force) must be zero.
Forces show inversion symmetry at opposite faces of the cell.

Net torque must be zero: Stress tensor symmetric.

$$X = \begin{pmatrix} \sigma_{11} & \sigma_{12} & \sigma_{13} \\ \sigma_{21} & \sigma_{22} & \sigma_{23} \\ \sigma_{31} & \sigma_{32} & \sigma_{33} \end{pmatrix} = \begin{pmatrix} \sigma_1 & \sigma_6 & \sigma_5 \\ * & \sigma_2 & \sigma_4 \\ * & * & \sigma_3 \end{pmatrix}$$

Landau-Lifshitz, Vol. 7, *Elasticity Theory*.
Wikipedia

Examples of stress tensors

Hydrostatic pressure

$$X = \begin{pmatrix} X & 0 & 0 \\ 0 & X & 0 \\ 0 & 0 & X \end{pmatrix}$$

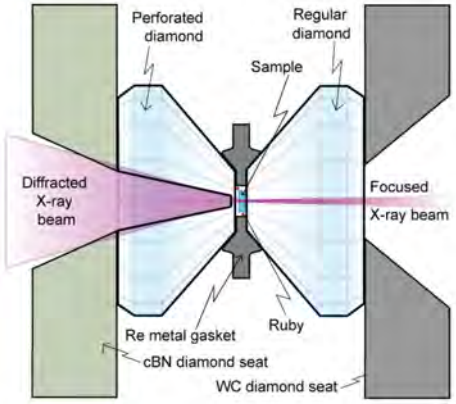

Diamond anvil cell

Uniaxial stress

$$X = \begin{pmatrix} X & 0 & 0 \\ 0 & 0 & 0 \\ 0 & 0 & 0 \end{pmatrix}$$

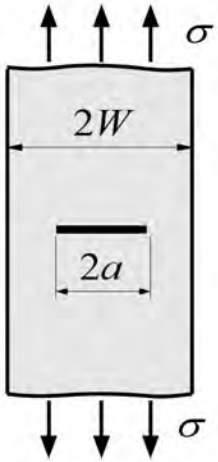

Thin rod in a vise

Biaxial stress

$$X = \begin{pmatrix} X & 0 & 0 \\ 0 & X & 0 \\ 0 & 0 & 0 \end{pmatrix}$$

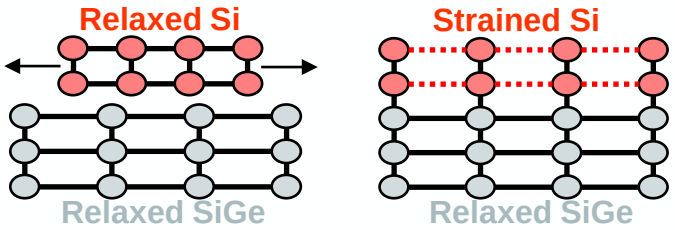

Pseudomorphic epitaxial layer

Landau-Lifshitz, Vol. 7, *Elasticity Theory*.
Google images

Measurement of wafer curvature (stress)

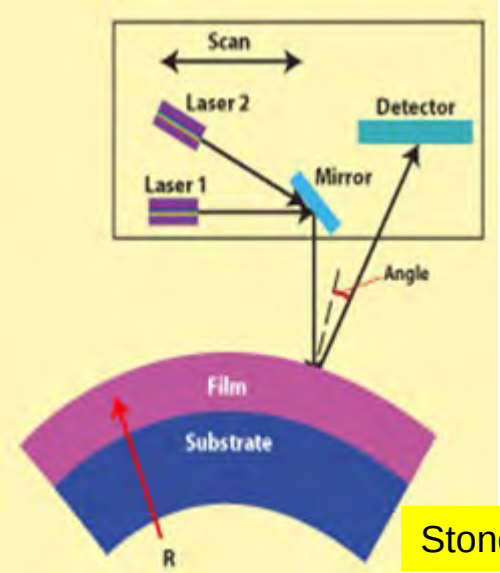

Flexus 2320-S
Dektak XT (stylus)

Stoney's Equation:

$$\sigma = \frac{T^2}{6Rt}\frac{E}{1-\nu}$$

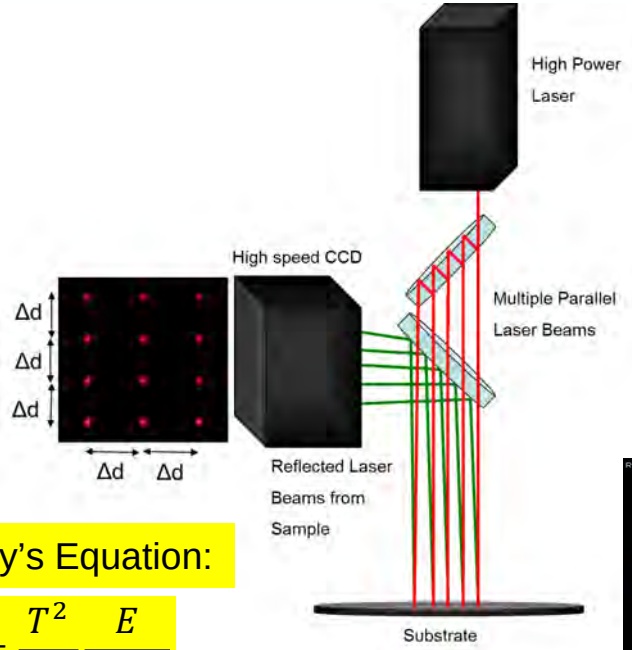

k-Space Associates, Inc.

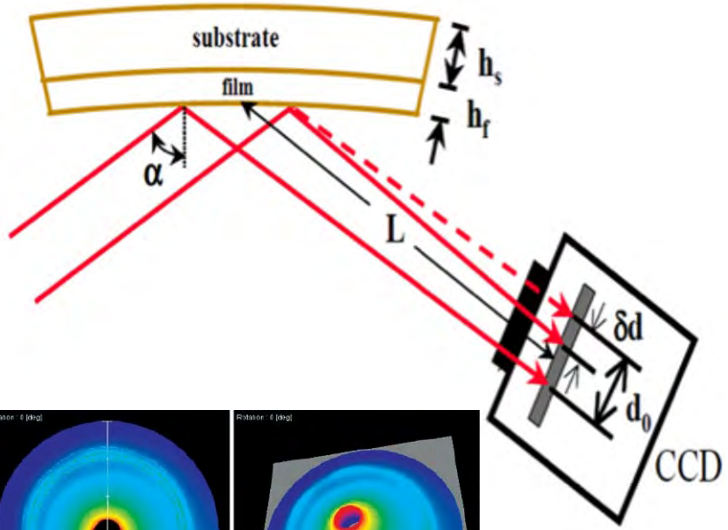

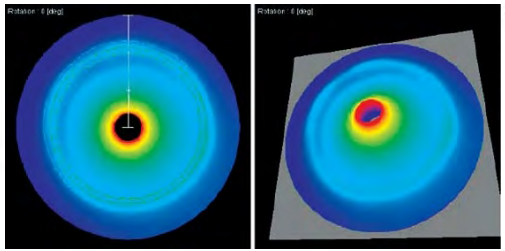

Measurement of stress with x-rays

Strain tensor

r Position of the unstrained point
r' Position of the strained point
u(**r**)=**r'**-**r** Displacement (vector field)

The **strain tensor** $\varepsilon(\mathbf{r})$ is defined by

$$\mathbf{u}(\mathbf{r})=\varepsilon(\mathbf{r})\mathbf{r}$$

This is a tensor field.
We assume a homogeneous strain $\varepsilon(\mathbf{r})=\varepsilon$.

Volume change:
$\Delta V/V=\mathrm{Tr}(\varepsilon)$
Poisson ratio: $(0<\nu<0.5)$

$$\nu = -\frac{\varepsilon_{11}}{\varepsilon_{33}}$$

$$\varepsilon = \begin{pmatrix} \varepsilon_{11} & \varepsilon_{12} & \varepsilon_{13} \\ \varepsilon_{21} & \varepsilon_{22} & \varepsilon_{23} \\ \varepsilon_{31} & \varepsilon_{32} & \varepsilon_{33} \end{pmatrix} = \begin{pmatrix} \varepsilon_1 & \varepsilon_6/2 & \varepsilon_5/2 \\ * & \varepsilon_2 & \varepsilon_4/2 \\ * & * & \varepsilon_3 \end{pmatrix}$$

Sign convention:
Positive ε: Tensile strain
Negative ε: Compressive strain

Onsager principle:
The strain tensor is **symmetric**.
It can be diagonalized (principal axes).

Determinant usually non-zero (Poisson ratio).

Landau-Lifshitz, Vol. 7, *Elasticity Theory*.

Examples of strain tensors

Group theory:
An arbitrary strain has a unique decomposition into a hydrostatic and (100) and (111) pure shear components.

Hydrostatic strain

$$\varepsilon_H = \begin{pmatrix} \varepsilon & 0 & 0 \\ 0 & \varepsilon & 0 \\ 0 & 0 & \varepsilon \end{pmatrix}$$

(001) uniaxial shear strain

$$\varepsilon_{(001)} = \begin{pmatrix} \varepsilon & 0 & 0 \\ 0 & \varepsilon & 0 \\ 0 & 0 & -2\varepsilon \end{pmatrix}$$

(111) uniaxial shear strain

$$\varepsilon_{(111)} = \begin{pmatrix} 0 & \varepsilon & \varepsilon \\ \varepsilon & 0 & \varepsilon \\ \varepsilon & \varepsilon & 0 \end{pmatrix}$$

Traceless: No volume change

Pressure P
Bulk modulus B (GPa)

$$B = -V\left(\frac{\partial V}{\partial P}\right)_T = \frac{P}{3\varepsilon}$$

In practical experimental geometries (uniaxial or biaxial stress) we usually find both hydrostatic and uniaxial shear components.

Strain measurements

$Ge_{1-y}Sn_y$ on GaAs (y=2.6%)

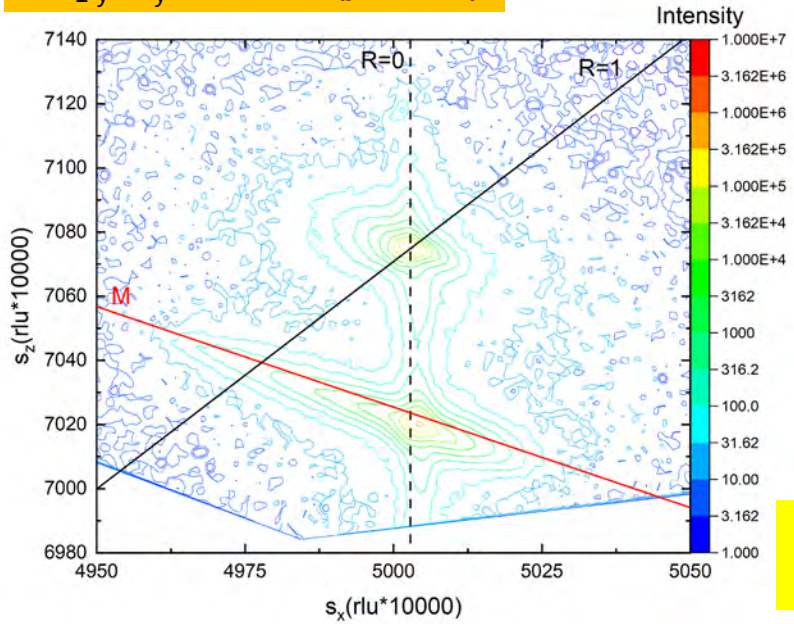

Asymmetric (224) grazing incidence reciprocal space map (XRD)

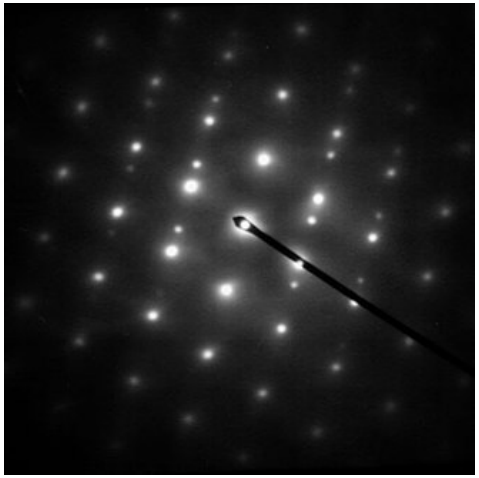

Transmission electron microscopy: Selected area diffraction

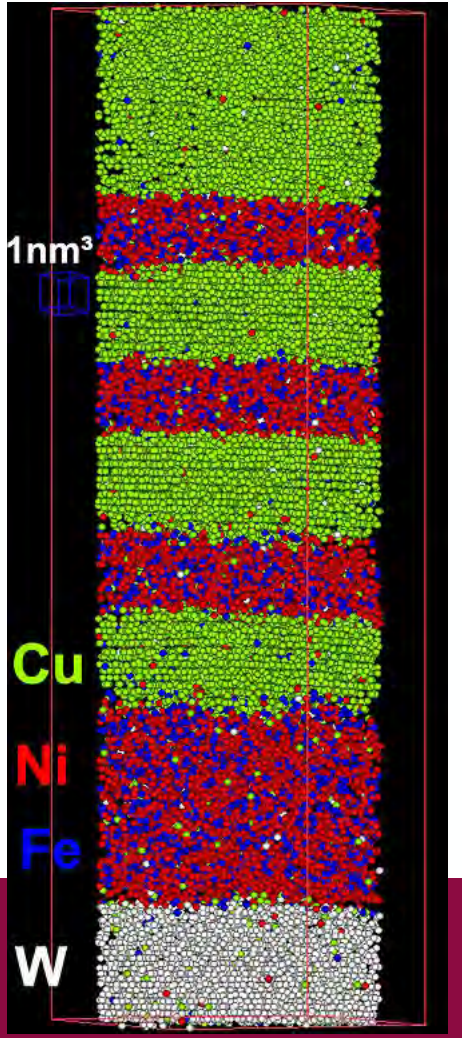

Atom probe tomography

Elasticity and compliance tensors (Hooke's Law)

Elasticity (stiffness) tensor c_{ijkl}

$$\sigma_{ij} = \sum_{kl} c_{ijkl}\varepsilon_{kl}$$

Compliance tensor S_{ijkl}

$$\varepsilon_{ij} = \sum_{kl} S_{ijkl}\sigma_{kl}$$

k,l=1..3

These are fourth rank-tensors with 81 elements.
Stress and strain tensors are symmetric, therefore only 21 elements are needed for *c* and *S*.

$$\sigma_i = \sum_{j} c_{ij}\varepsilon_j$$

i,j=1..6

$$s_{lm} = \begin{cases} S_{ijkl} & \text{if} \quad l,m < 3 \\ 2S_{ijkl} & \text{if} \quad \text{mixed} \\ 4S_{ijkl} & \text{if} \quad l,m > 3 \end{cases}$$

No factors of 2,4 for c_{ij}.

6x6 matrices are symmetric: 21 elements

$$\varepsilon_i = \sum_{j} s_{ij}\sigma_j$$

i,j=1..6

Compliance tensors for different symmetries

The number of independent elements of the compliance tensor is reduced further by crystal symmetry.
Triclinic system: 21 elements

Cubic system: We only have three elements: s_{11}, s_{12}, s_{44}

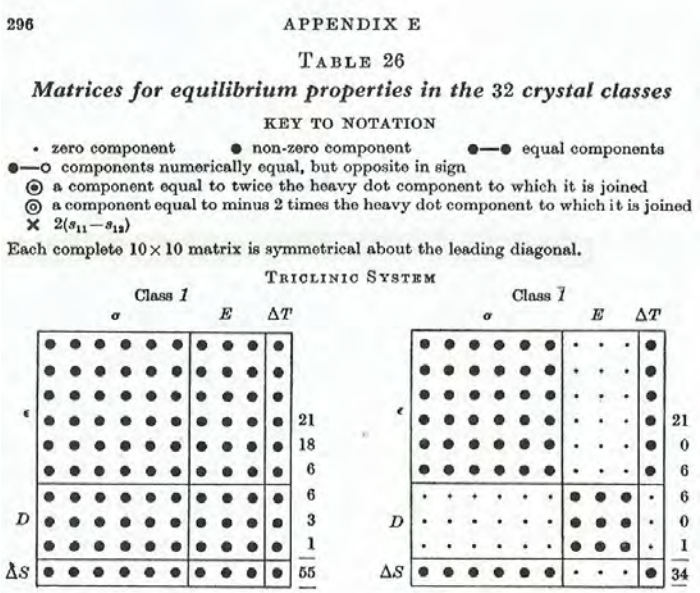

296 APPENDIX E

TABLE 26

Matrices for equilibrium properties in the 32 crystal classes

KEY TO NOTATION

• zero component ● non-zero component ●—● equal components
●—○ components numerically equal, but opposite in sign
◉ a component equal to twice the heavy dot component to which it is joined
◎ a component equal to minus 2 times the heavy dot component to which it is joined
× $2(s_{11}-s_{12})$

Each complete 10×10 matrix is symmetrical about the leading diagonal.

TRICLINIC SYSTEM

Class *1* — Class $\bar{1}$

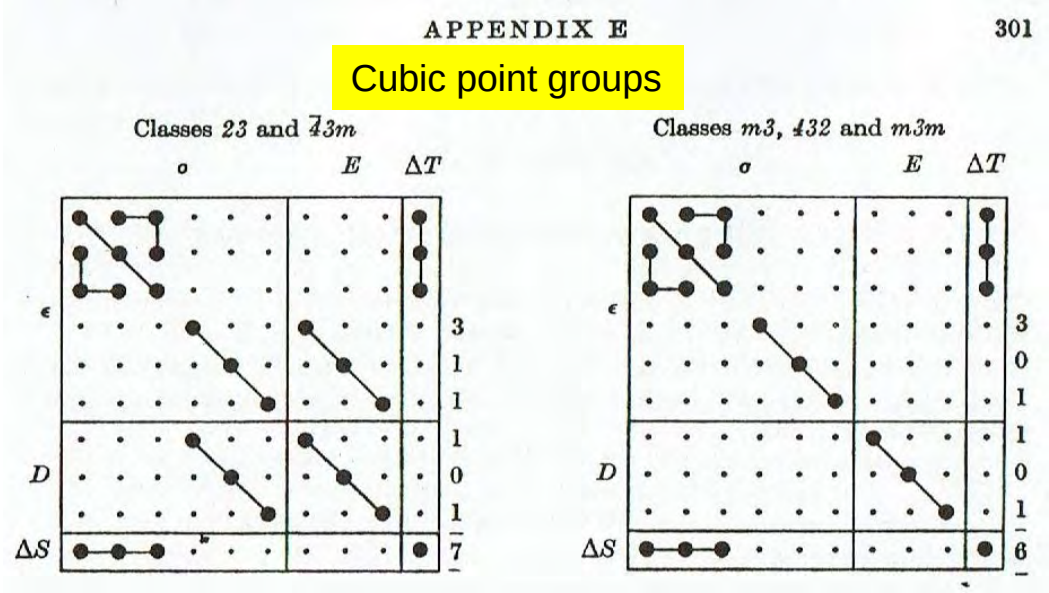

APPENDIX E 301

Cubic point groups

Classes *23* and $\bar{4}3m$ — Classes *m3*, *432* and *m3m*

Phonon spectra under uniaxial strain

Uniaxial strain splits the three-fold degenerate Raman phonon in Si into a singlet and a triplet.

$$\varepsilon = \begin{pmatrix} \varepsilon_{\parallel} & 0 & 0 \\ 0 & \varepsilon_{\parallel} & 0 \\ 0 & 0 & \varepsilon_{\perp} \end{pmatrix}$$

For this strain tensor, the stress could be uniaxial or biaxial along (100).

$$\Omega_s = \omega_0 + \frac{1}{2\omega_0}(p\varepsilon_{\perp} + 2q\varepsilon_{\parallel})$$

$$\Omega_d = \omega_0 + \frac{1}{2\omega_0}[p\varepsilon_{\parallel} + q(\varepsilon_{\parallel} + \varepsilon_{\perp})]$$

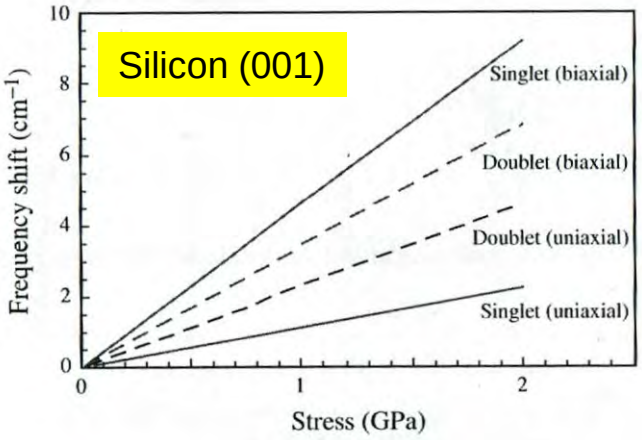

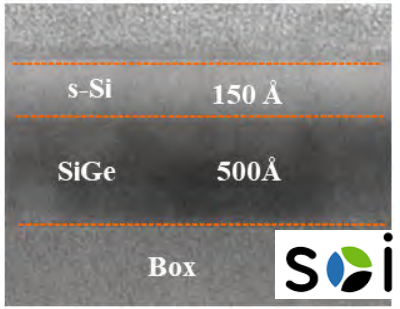

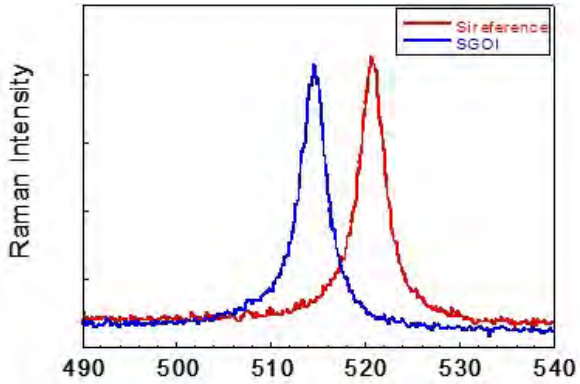

Only the singlet is observable in conventional backscattering geometry.

R. Liu and N. Cave in Pantelides and Zollner: *Silicon-Germanium-Carbon Alloys*.

UV Raman stress mapping in Si devices

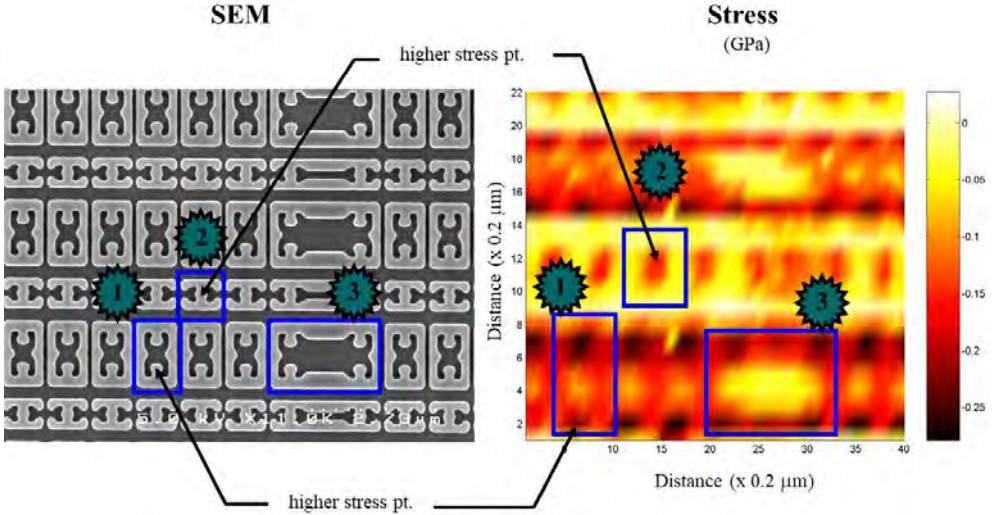

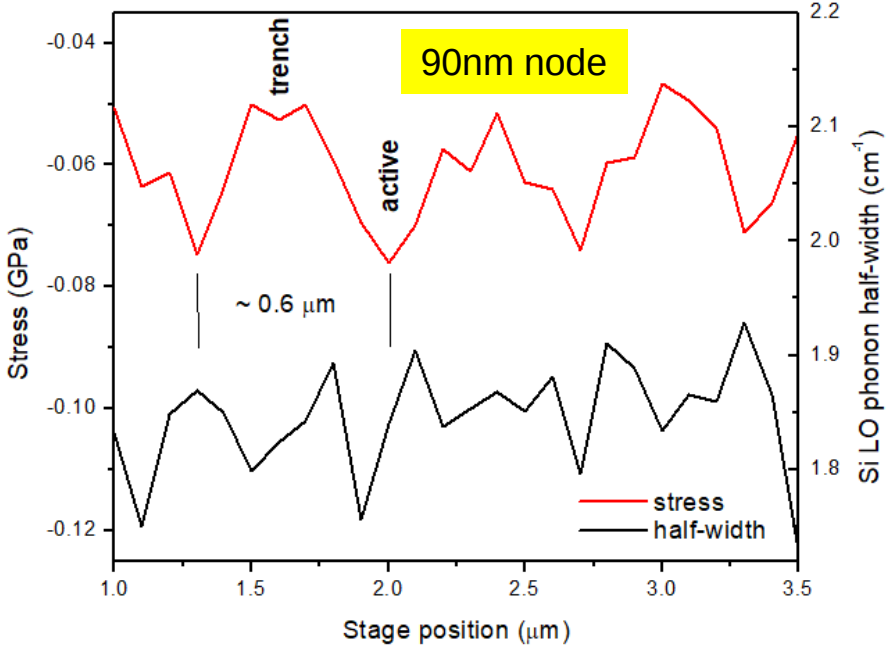

325 nm He-Cd laser, 0.4 μm spot size
UV-enhanced spectrometer

Useful for devices with half-pitch greater than 0.13 μm
Obsolete since around 2002.

UV Raman stress measurements in group-IV alloys

Strain and composition effects on Raman vibrational modes of silicon-germanium-tin ternary alloys

J.-H. Fournier-Lupien,[1] S. Mukherjee,[1] S. Wirths,[2] E. Pippel,[3] N. Hayazawa,[1,a)] G. Mussler,[2] J. M. Hartmann,[4] P. Desjardins,[1] D. Buca,[2] and O. Moutanabbir[1,b)]
[1]*Department of Engineering Physics, École Polytechnique de Montréal, Montréal, C. P. 6079, Succ. Centre-Ville, Montréal, Québec H3C 3A7, Canada*
[2]*Peter Grünberg Institute 9 and JARA-FIT, Forschungszentrum Juelich, 52425 Juelich, Germany*
[3]*Max Planck Institute of Microstructure Physics, Weinberg 2, Halle (Saale) 06120, Germany*
[4]*CEA, LETI, Minatec Campus, 17 rue des Martyrs, 38054 Grenoble, France*

(Received 4 November 2013; accepted 8 December 2013; published online 26 December 2013)

We investigated Raman vibrational modes in silicon-germanium-tin layers grown epitaxially on germanium/silicon virtual substrates using reduced pressure chemical vapor deposition. Several excitation wavelengths were utilized to accurately analyze Raman shifts in ternary layers with uniform silicon and tin content in 4–19 and 2–12 at. % ranges, respectively. The excitation using a 633 nm laser was found to be optimal leading to a clear detection and an unambiguous identification of all first order modes in the alloy. The influence of both strain and composition on these modes is discussed. The strain in the layers is evaluated from Raman shifts and reciprocal space mapping data and the obtained results are discussed in the light of recent theoretical calculations. © *2013 AIP Publishing LLC*. [http://dx.doi.org/10.1063/1.4855436]

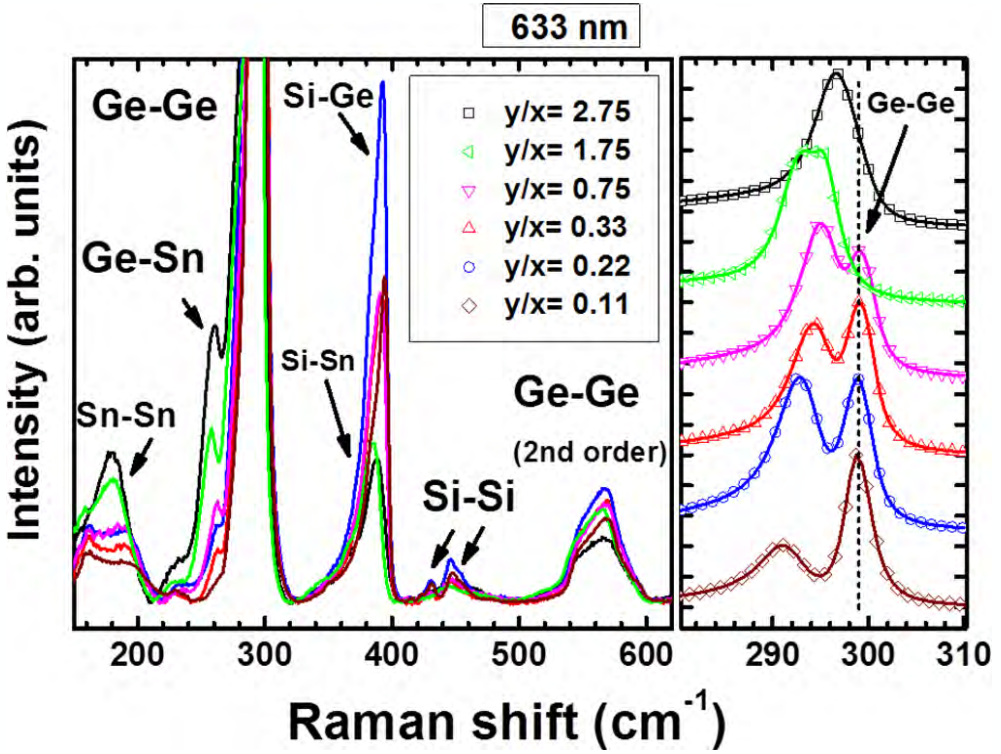

Raman spectroscopy is useful to determine the composition of Si-Ge-Tin alloys, but strain must be subtracted in the analysis.

Electronic bands under hydrostatic strain

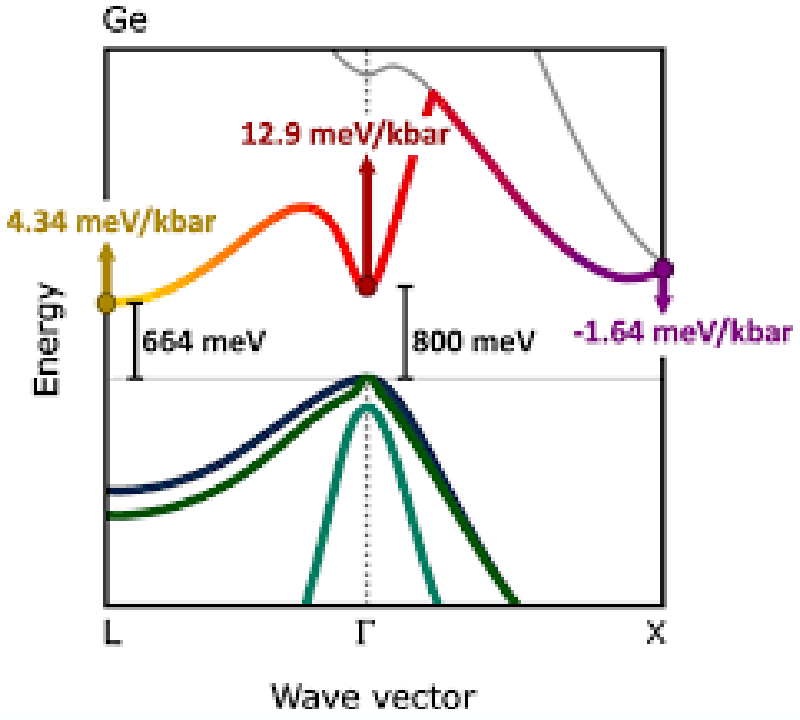

Deformation potential:

$$D_{n\vec{k}} = \frac{\partial E_{n\vec{k}}}{\partial \vec{r}}$$
$$\Delta E_{n\vec{k}} = D_{n\vec{k}} f(\varepsilon)$$

Valence bands remain about the same.
(Deformation potential a_V is small.)

Conduction bands:
Γ-point moves up fast (a_C=–10 eV).
L-point also moves up (Ge becomes more indirect).
X-point moves down (GaAs becomes indirect at 41 kbar).

Paul's rule:
Deformation potentials do not vary much between semiconductor materials for the same band or transition.

Valence bands of Si under (001) stress

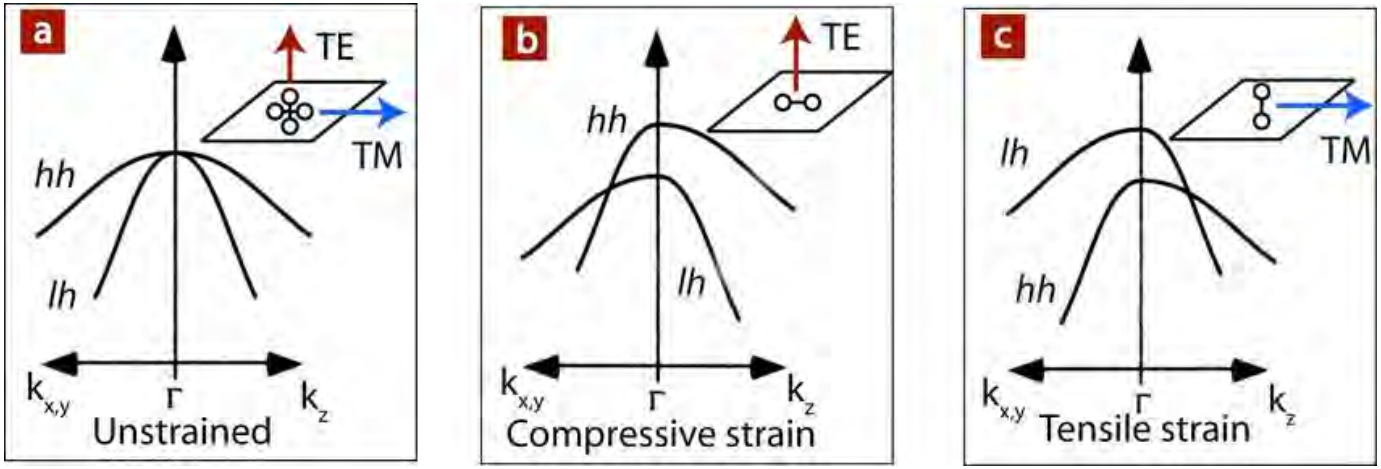

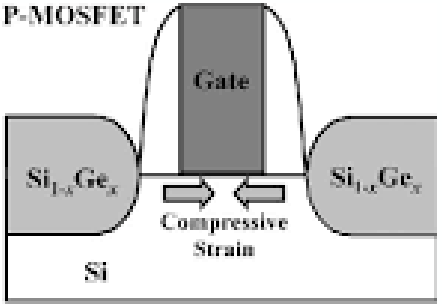

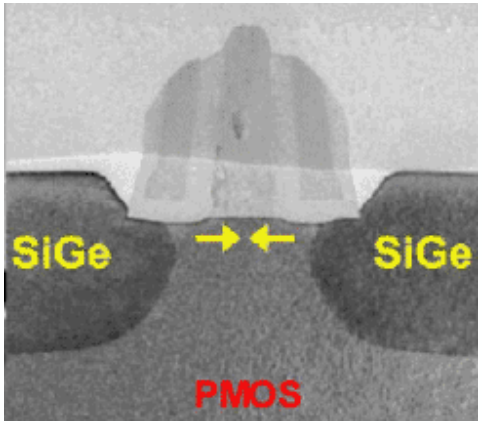

A uniaxial compressive stress is created by embedded Si-Ge source-drain stressors.
Under compressive uniaxial stress, the hole mobility increases.
This technology is used for most high-performance PMOS transistors.

Pantelides and Zollner,
Silicon-Germanium-Carbon Alloys.

Conduction bands of Si under (001) stress

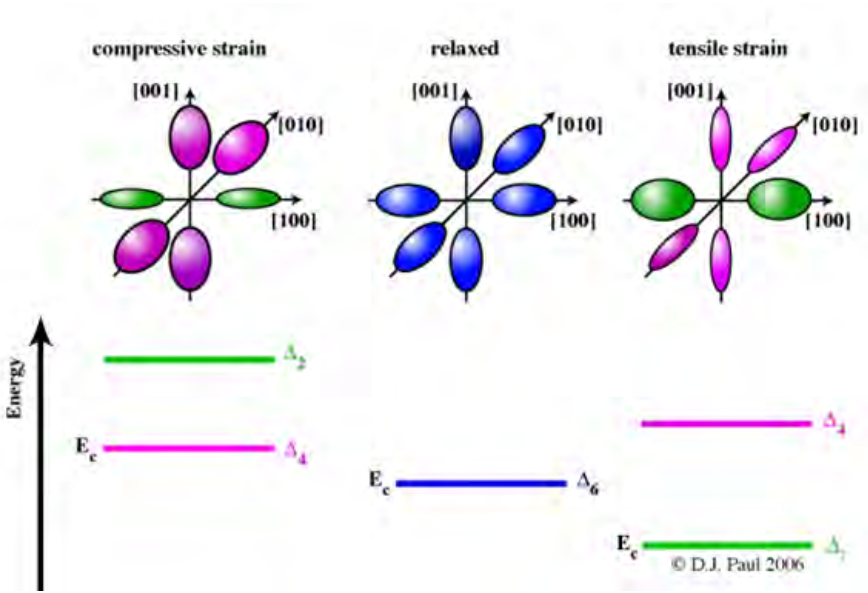

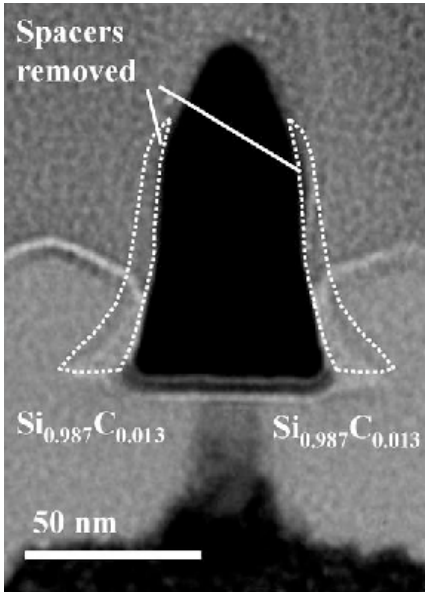

A uniaxial compressive stress splits the six-fold degenerate conduction band valleys of Si.
This reduces the f- and g-intervalley scattering and also changes the effective masses.
This can be achieved with tensile nitride stress liners or with embedded Si-C alloy stressors.

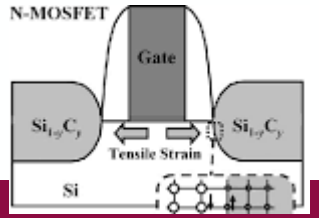

Pantelides and Zollner,
Silicon-Germanium-Carbon Alloys.

Photoluminescence of $Si_{1-x}Ge_x$ alloys on Si

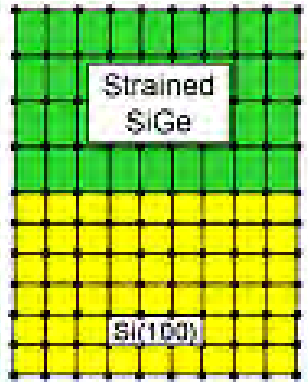

Pseudomorphic growth of $Si_{1-x}Ge_x$ alloy on Si (001)

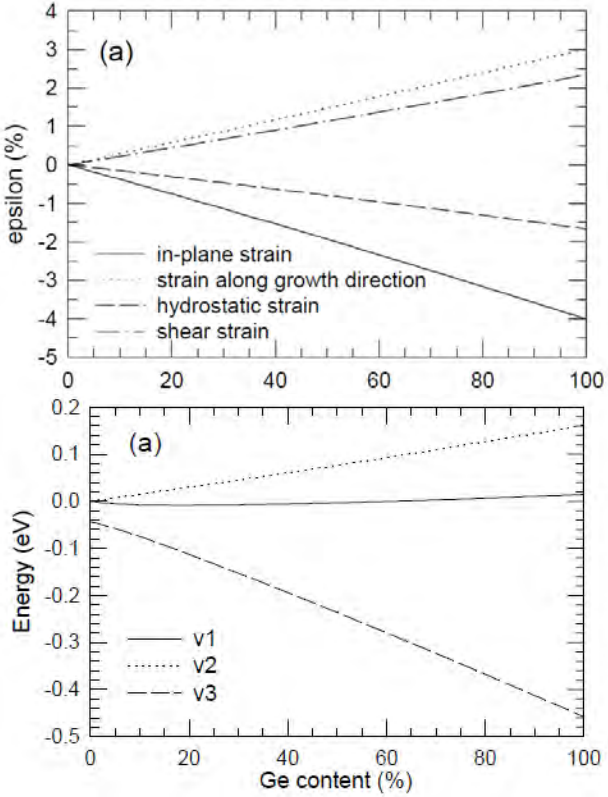

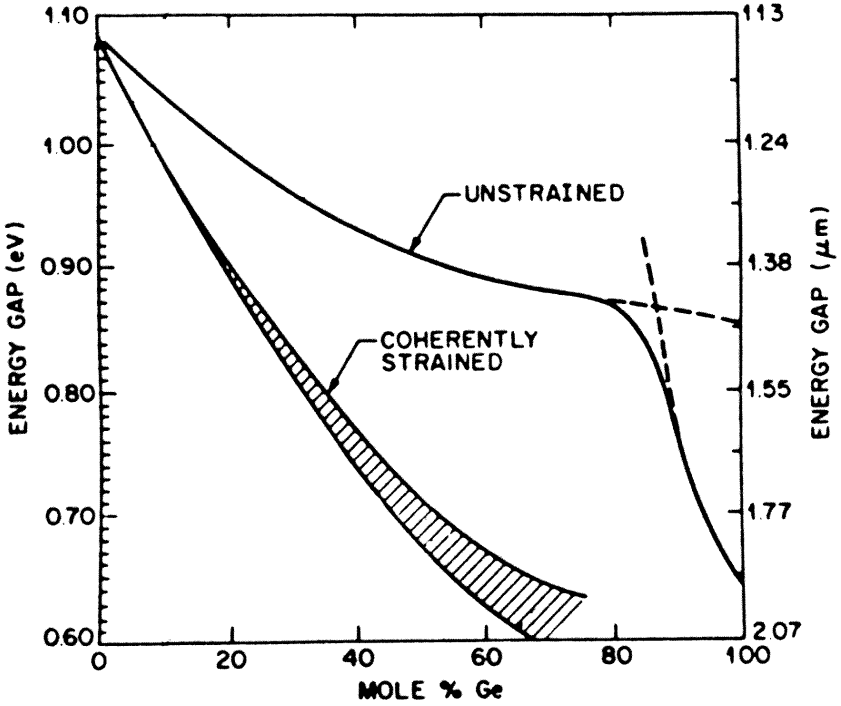

Pantelides and Zollner, *Silicon-Germanium-Carbon Alloys*.

Strain splitting of E_1 and $E_1+\Delta_1$ transitions

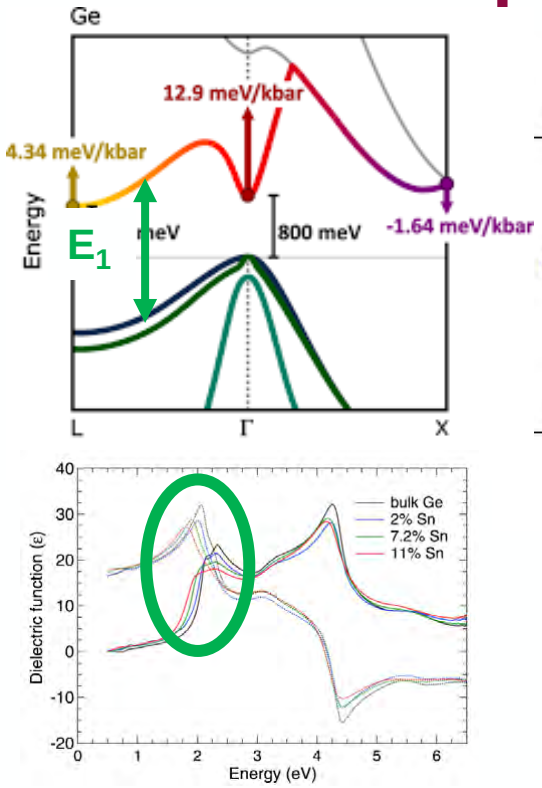

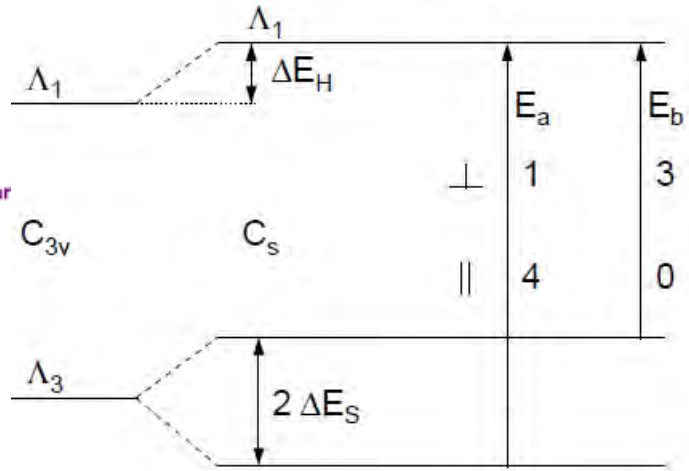

Large shear approximation
(small spin-orbit splitting)

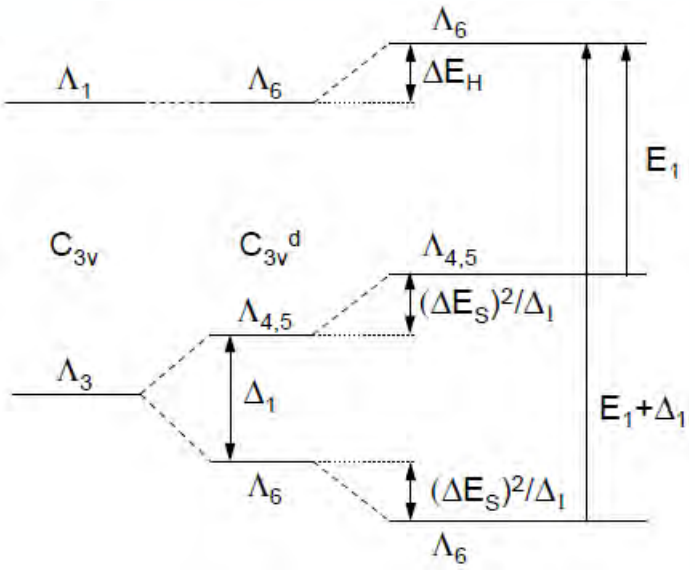

Small shear approximation
(large spin-orbit splitting)

Pantelides and Zollner,
Silicon-Germanium-Carbon Alloys.

Spectroscopic ellipsometry

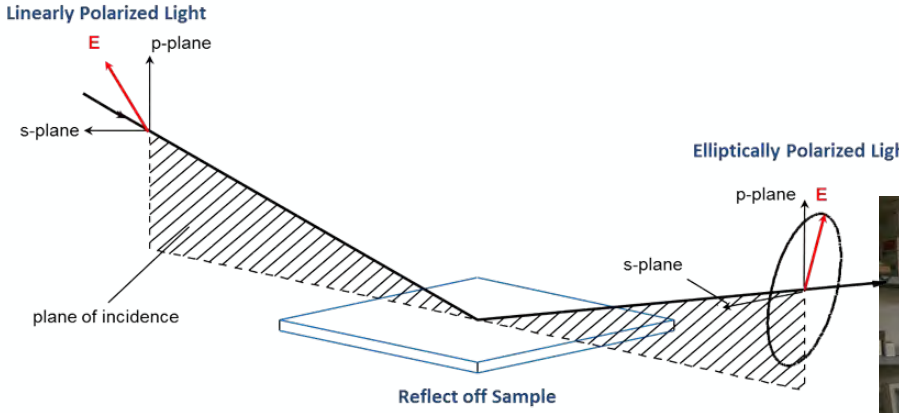

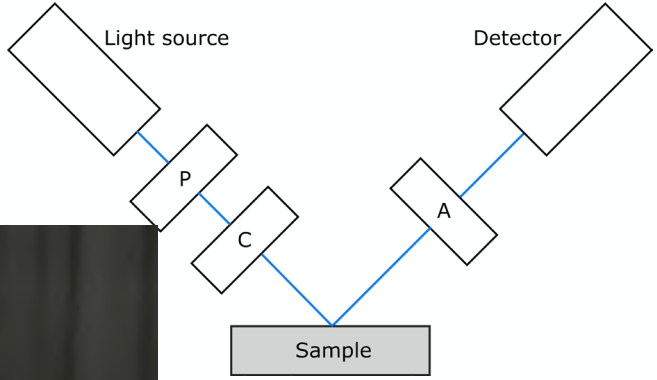

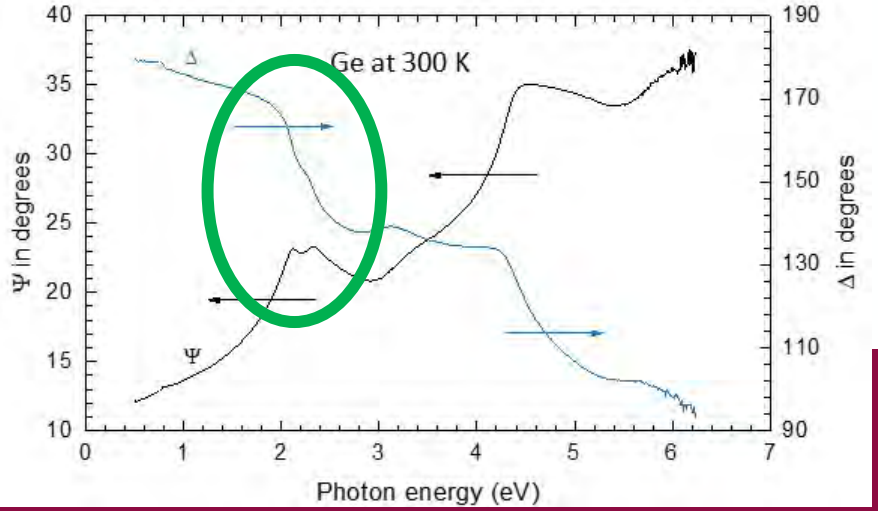

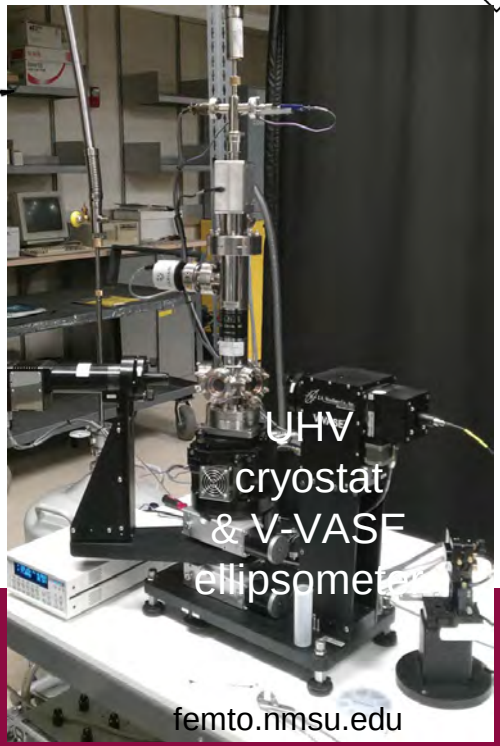

$$\rho = \frac{r_p}{r_s} = \tan\Psi\, e^{i\Delta}$$

Ellipsometry instrumentation

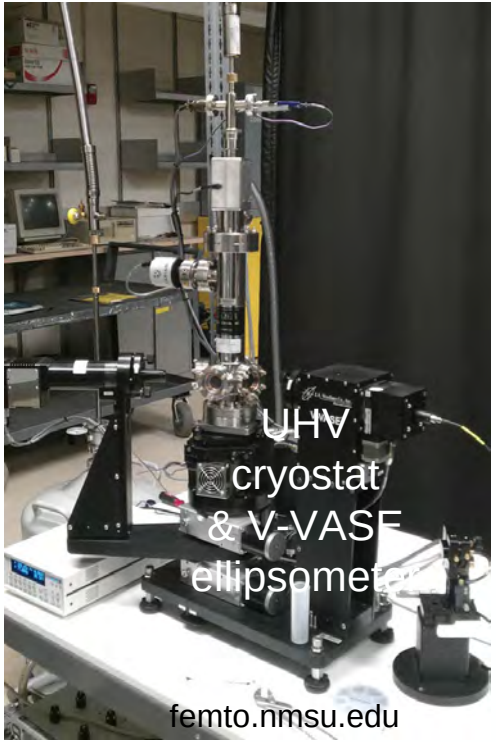

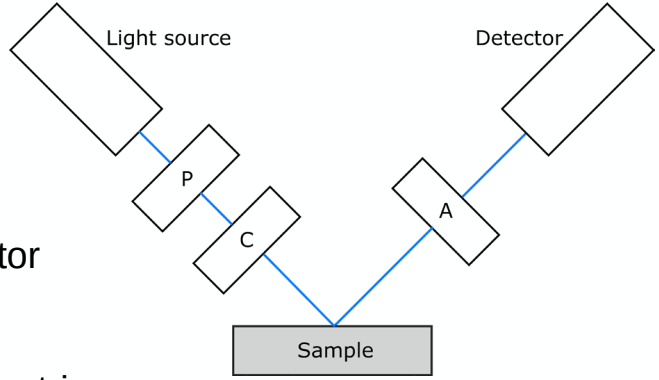

Broadband versus scanning monochromator
FTIR and near-IR/VIS/near-UV
Compensator is crucial for small Δ
Dual rotating compensators: Full Mueller matrix

Option: Phase-modulation ellipsometry

Equidistant energies or wavelengths

Spot size: 10 mm or 30 μm on 1 μm (imaging)

Penetration depth

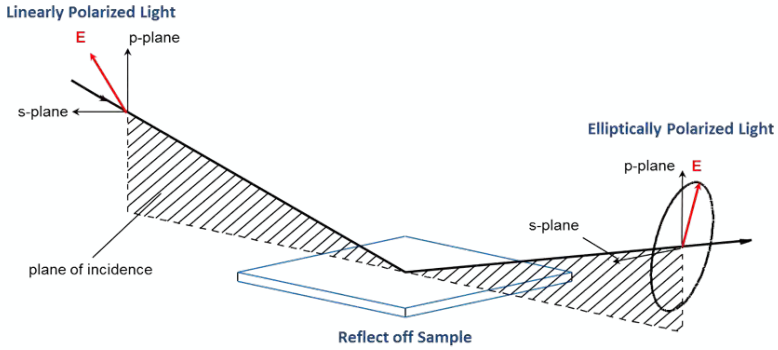

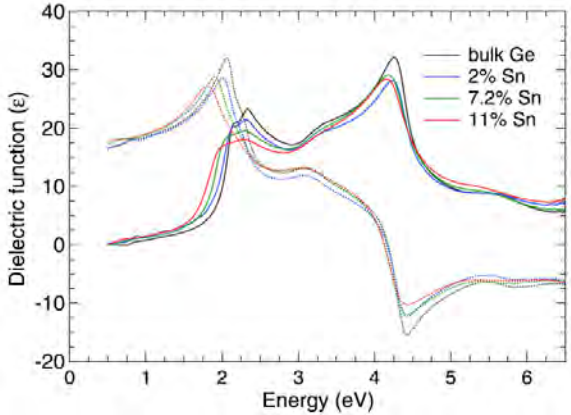

The penetration depth is the inverse of the absorption coefficient, which can be measured with spectroscopic ellipsometry.

Below the direct band gap (0.8 eV for Ge, 3.4 eV for Si), the penetration depth is very large (many microns).

The penetration depth is smallest at the E_2 peak in the UV, about 10 nm.

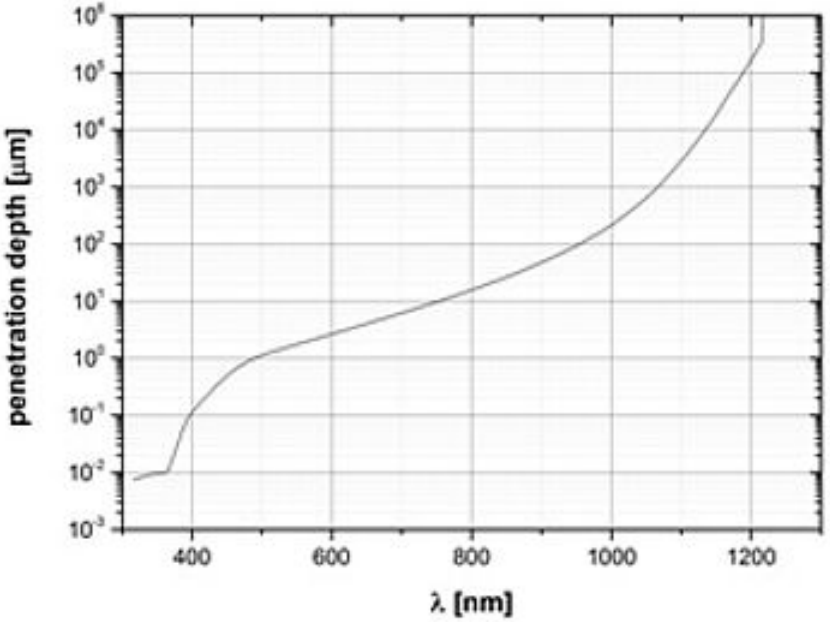

Critical points in the dielectric function of Ge

- Structures in the dielectric function
- Due to interband transitions

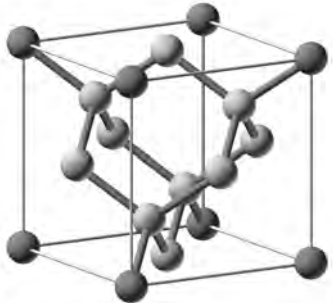

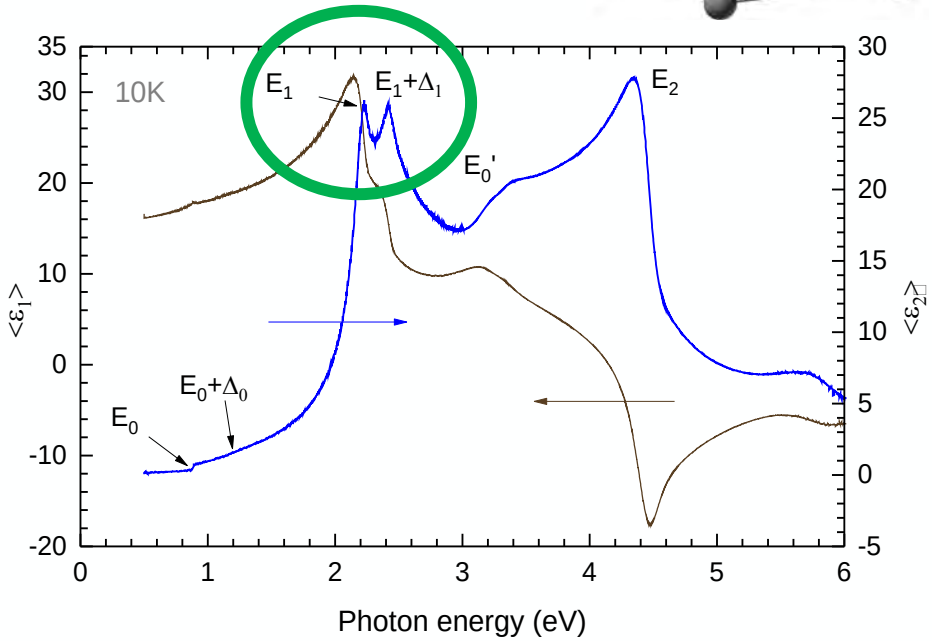

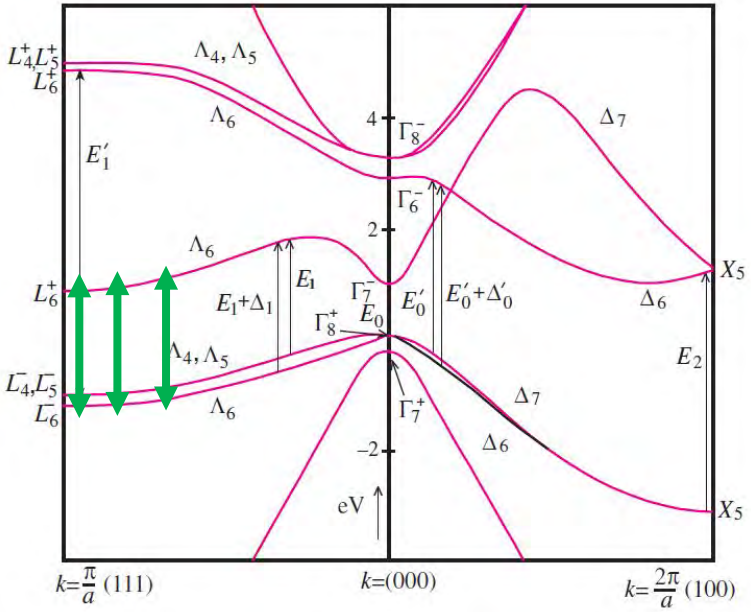

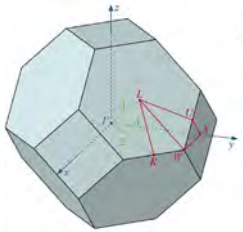

P.Y. Yu and M. Cardona,
Fundamentals of Semiconductors.

Piezo-optics of Si, Ge, GaAs under (001) strain

Elasto-optical constants of **Si**
P. Etchegoin, J. Kircher, and M. Cardona
Phys. Rev. B 47, 10292 (1993).

Piezo-optics of **GaAs**
P. Etchegoin, J. Kircher, M. Cardona, C. Grein, and E. Bustarret
Phys. Rev. B 46, 15139 (1992).

Piezo-optical response of **Ge** in the visible–uv range
P. Etchegoin, J. Kircher, M. Cardona, and C. Grein
Phys. Rev. B 45, 11721 (1992).

Piezo-optics of **InP** in the visible-ultraviolet range
D. Rönnow, P. Santos, M. Cardona, E. Anastassakis, and M. Kuball
Phys. Rev. B 57, 4432 (1998: E: 1999).

Etienne Bustarret

Tensile biaxial stress in Ge layers on Si

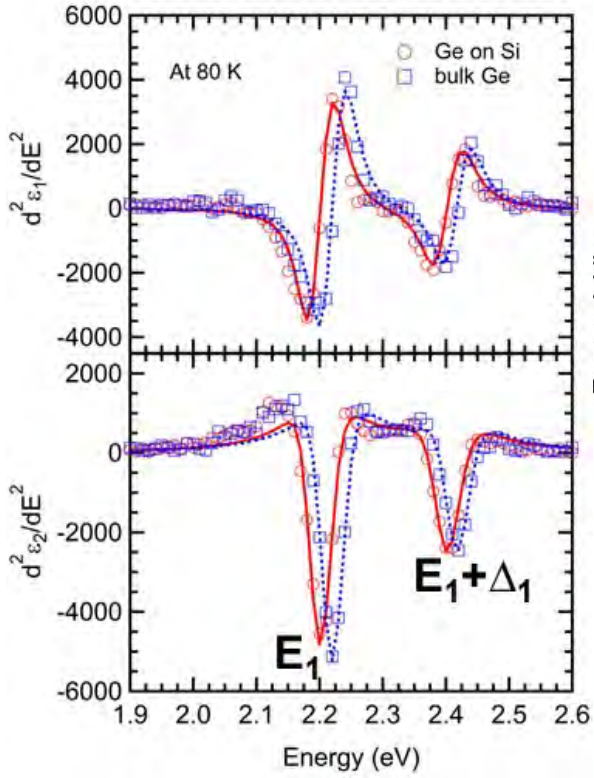

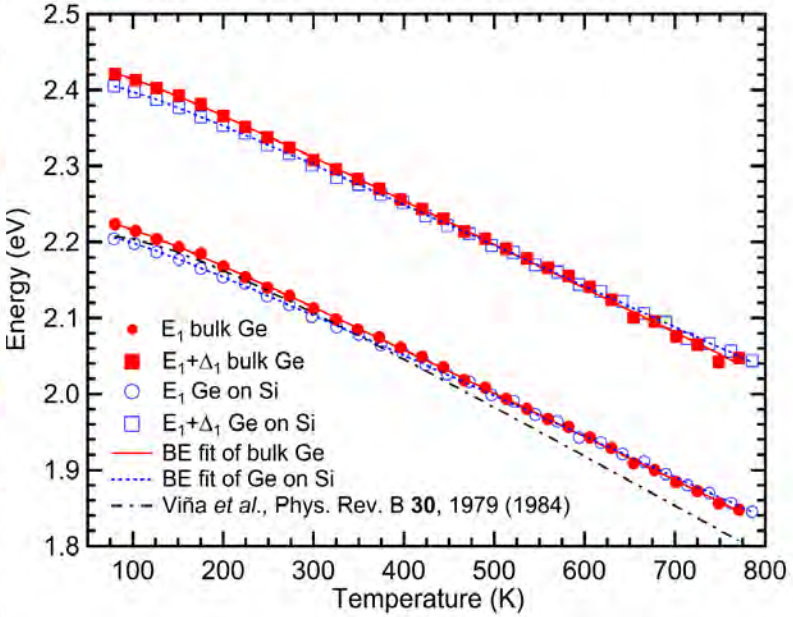

1 meV accuracy for E_1 energy measurement.

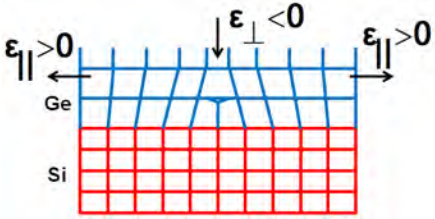

$$\varepsilon_{||}(T) = \int_{T_1}^{T_g} [\alpha_{Ge}(T) - \alpha_{Si}(T)]dT$$

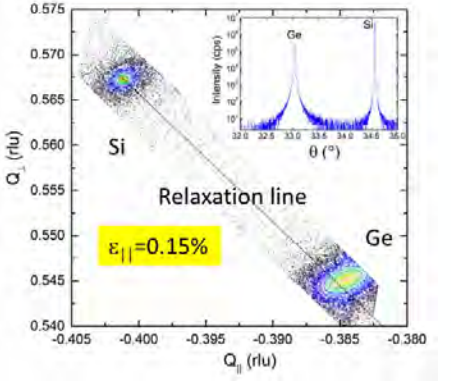

Optical and X-Ray Characterization of $Ge_{1-y}Sn_y$ alloys on GaAs

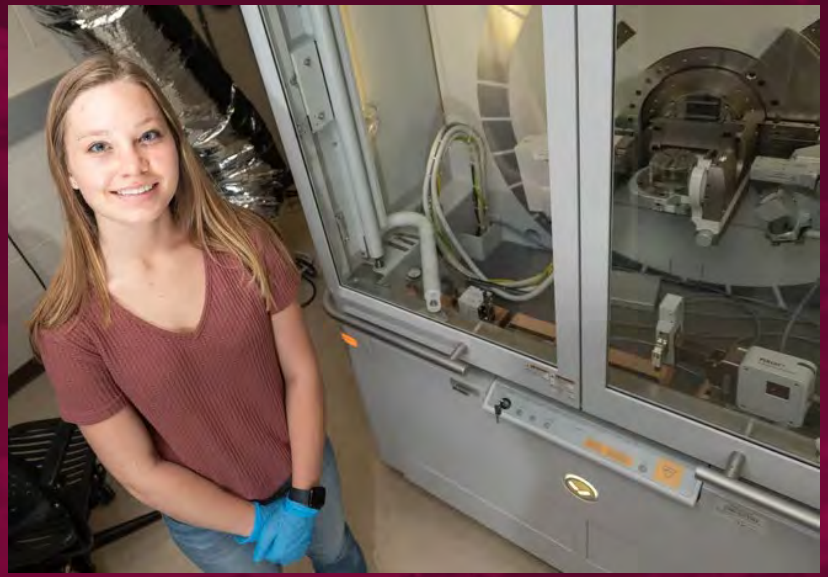

Haley B. Woolf,[1] Matt Kim,[2] Carola Emminger,[1] Carlos A. Armenta,[1] Stefan Zollner[1]

1. Department of Physics, New Mexico State University, Las Cruces, NM, USA
2. QuantTera, Scottsdale, AZ, USA

2022 AVS International Symposium, Pittsburgh, PA, USA. November 2023.

This work was supported by Air Force Office of Scientific Research under award number FA9550-20-1-0135.

Outline

- Introduction
- X-ray diffraction data:
  - Omega scans (rocking curves), and reciprocal space maps on (004), (224), & $(\bar{2}\bar{2}4)$ reflections
- Composition and lattice constant
- Optical data:
  - Pseudodielectric function, optical constants, and second derivative spectra
  - Photoluminescence data: dependence of E_0 on tin content
- Dependence of E_1 and $E_1+\Delta_1$ on tin content (ellipsometry)
- Conclusion

Introduction

- GeSn alloys with tunable bandgaps are of interest for **mid infrared lasers and detectors**. They can be integrated with common semiconductor substrates (Si, Ge, GaAs).
- Two **$Ge_{1-y}Sn_y$ layers** were grown **on GaAs** by **chemical vapor epitaxy** with different amounts of tin. The tin content is found with (004) omega rocking curves and reciprocal space maps.
- The tin contents were found to be 1.2% and 2.6% with thicknesses of 1600 Å and 1150 Å, respectively.
- Asymmetric (224) grazing incidence and $(\bar{2}\bar{2}4)$ grazing exit reciprocal space maps were used to determine the strain and relaxation of the epitaxial layer.
- From the dielectric function and the tin content, we can compare the E_1 and $E_1+\Delta_1$ energies with continuum elasticity theory. When the tin content increases, the energies decrease.
- Photoluminescence data was taken of both samples and compared to bulk Ge to observe the change in E_0. Using continuum elasticity theory for E_0, we see that when the tin content increases, the energies decrease.

(004) Rocking Curves: Strained or relaxed ???

ω Scan Open Detector:

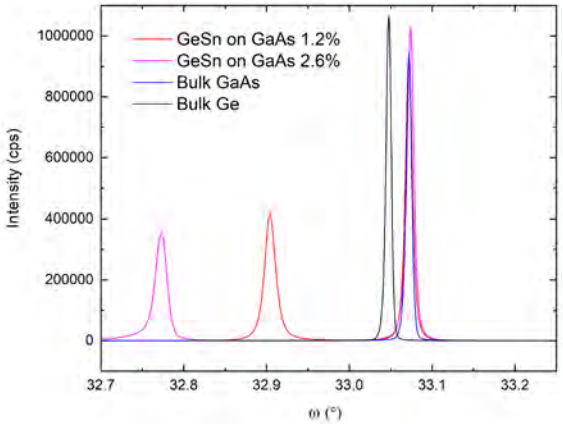

FWHM	
GaAs	0.010°
GeSn	0.016°
GaAs	0.010°
GeSn	0.017°
Bulk GaAs	0.0077°
Bulk Ge	0.0074°

Taken at 2θ = 66.4240°

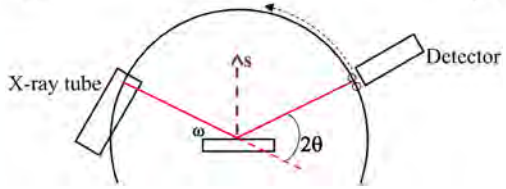

ω-2θ Scan Open Detector:

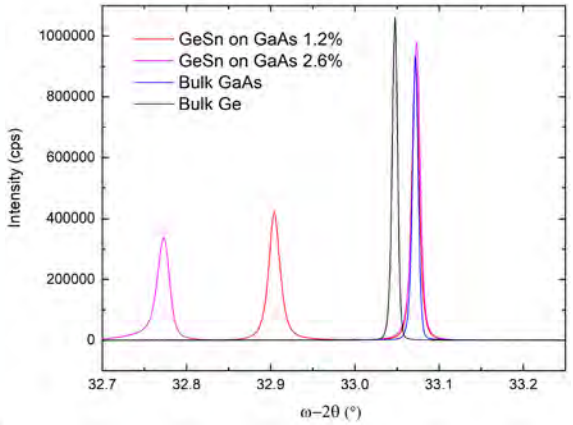

	FWHM
GaAs	0.010°
GeSn	0.016°
GaAs	0.010°
GeSn	0.017°
Bulk GaAs	0.0078°
Bulk Ge	0.0074°

Vertical Lattice Constants:

GaAs:	5.652 Å
GeSn:	5.679 Å
GaAs:	5.652 Å
GeSn:	5.699 Å
Bulk GaAs:	5.653 Å
Bulk Ge:	5.658 Å

Even the GaAs substrate is broader if an epilayer has been grown (dislocations may penetrate from the epilayer into the substrate).

(004) Reciprocal Space Maps

Bulk GaAs

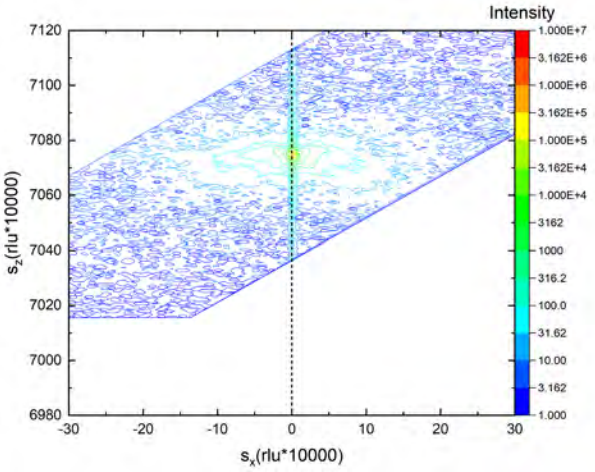

Bulk Ge

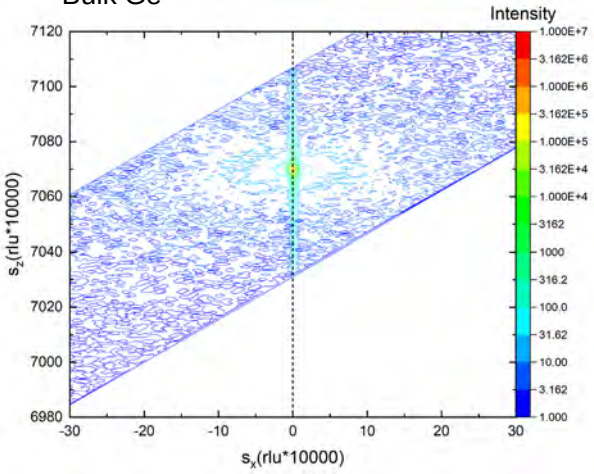

GeSn on GaAs 1.2%

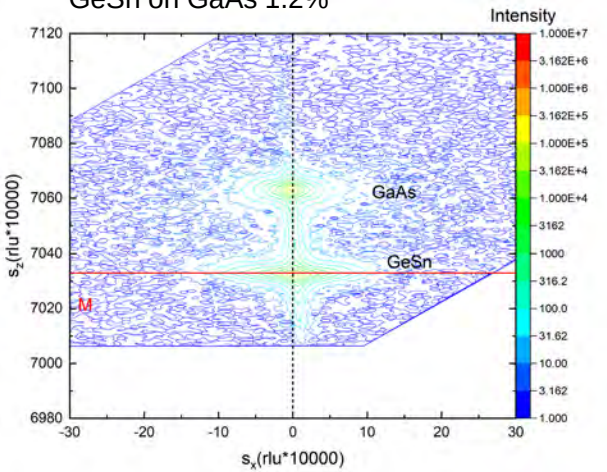

GeSn on GaAs 2.6%

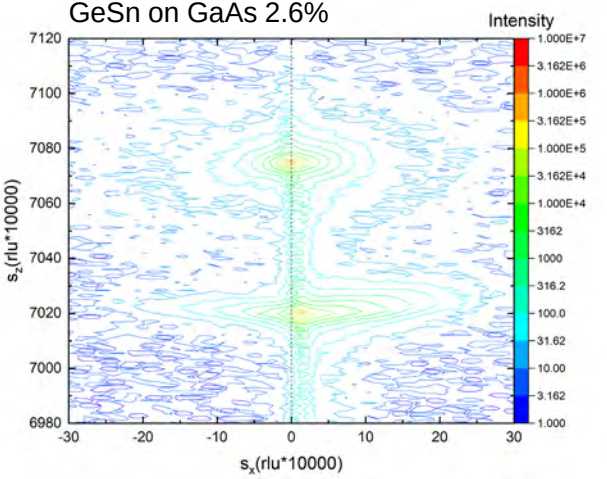

Dashed line drawn through substrate peak

M-Mosaic Spread (Relaxation Line)

No tilt between epilayer and substrate.

$$s_x = \frac{q_x}{2\pi} = \frac{1}{\lambda}[\cos(\omega) - \cos(2\theta - \omega)]$$

$$s_z = \frac{q_z}{2\pi} = \frac{1}{\lambda}[\sin(\omega) + \sin(2\theta - \omega)]$$

$$\lambda = 1.5406\ \text{Å}$$

$(\bar{2}\bar{2}4)$ & (224) Rocking Curve (Open Detector)

$(\bar{2}\bar{2}4)$ Grazing Exit

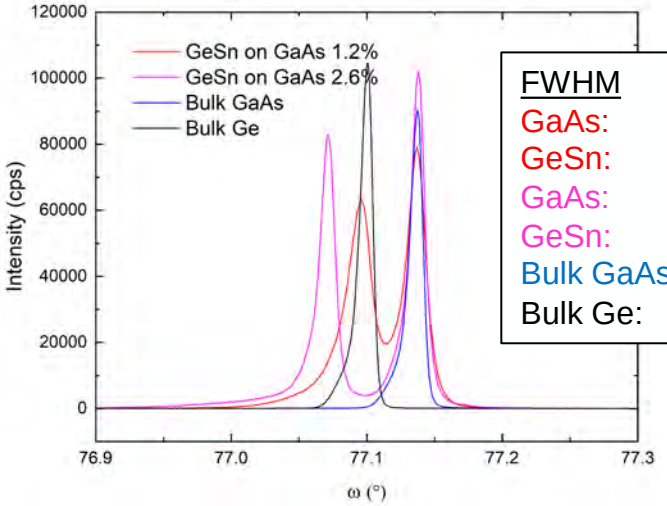

FWHM	
GaAs:	0.017°
GeSn:	0.022°
GaAs:	0.013°
GeSn:	0.013°
Bulk GaAs:	0.011°
Bulk Ge:	0.011°

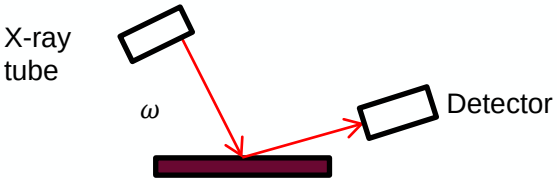

(224) Grazing Incidence

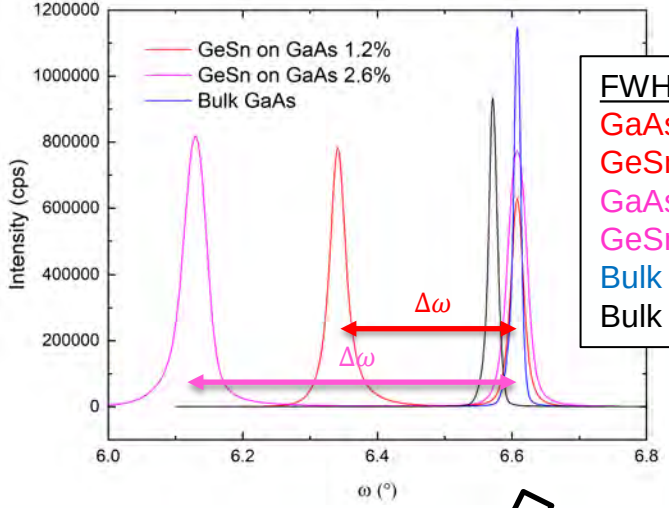

FWHM	
GaAs:	0.022°
GeSn:	0.028°
GaAs:	0.033°
GeSn:	0.041°
Bulk GaAs:	0.013°
Bulk Ge:	0.015°

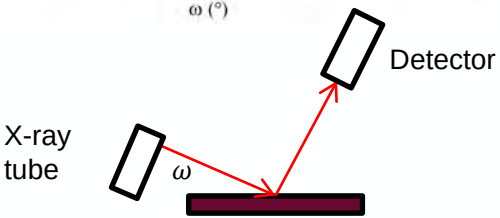

Haley B. Woolf et al., 2022 AVS Symposium, Pittsburgh, PA, USA. November 2023.

(224) Grazing Incidence RSM

Bulk GaAs

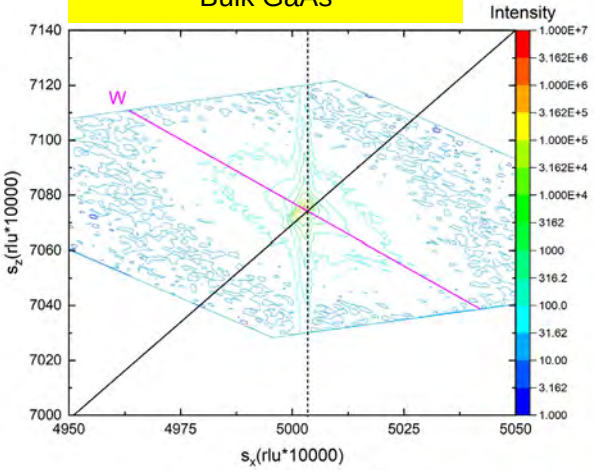

Bulk Ge

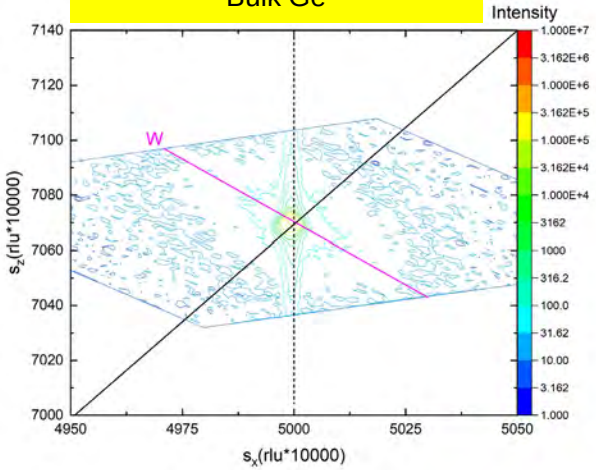

GeSn on GaAs 1.2%

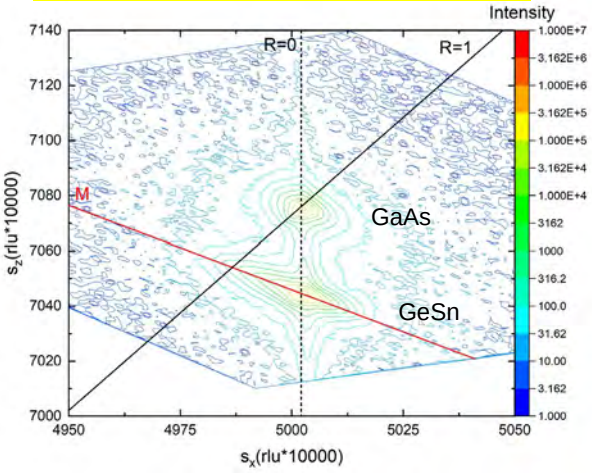

GeSn on GaAs 2.6%

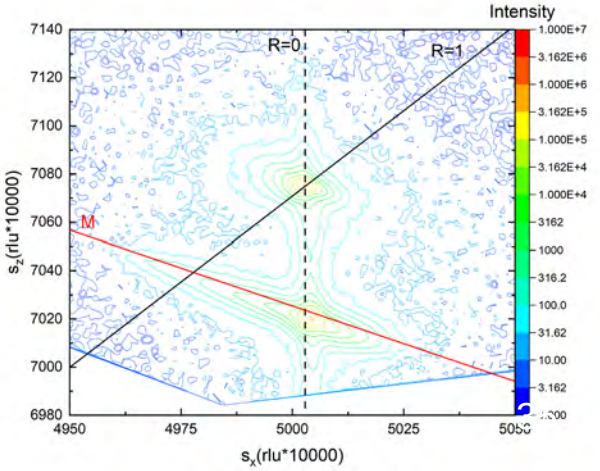

W-Wavelength Streak

M-Mosaic Spread (Relaxation Line)

Black line drawn from origin (Relaxed)

Dashed line drawn through substrate peak (Pseudomorphic)

$$s_x = \frac{q_x}{2\pi} = \frac{1}{\lambda}[\cos(\omega) - \cos(2\theta - \omega)]$$

$$s_z = \frac{q_z}{2\pi} = \frac{1}{\lambda}[\sin(\omega) + \sin(2\theta - \omega)]$$

$$\lambda = 1.5406\ \text{Å}$$

Lattice Constants

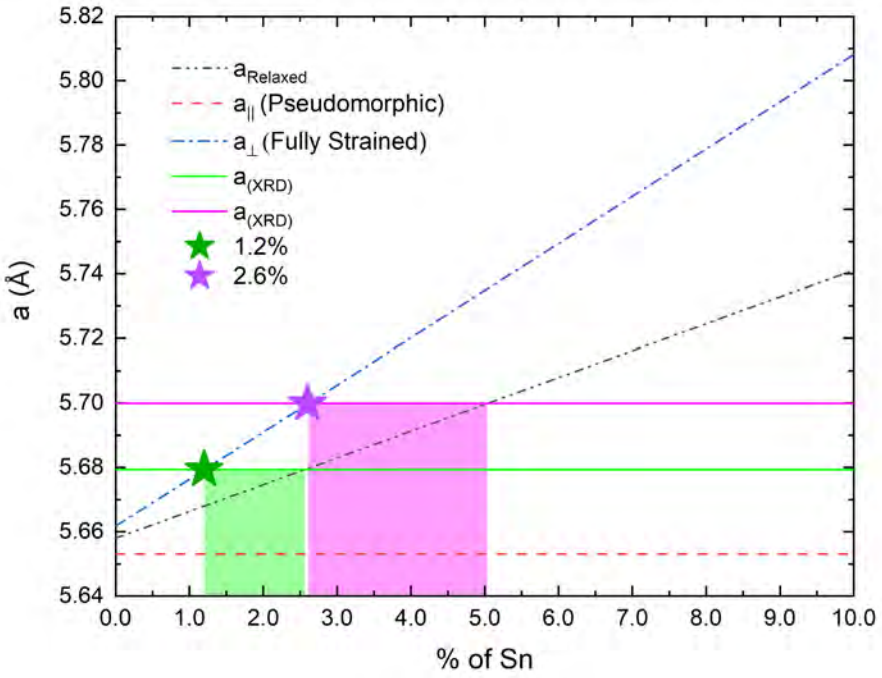

Bragg's Law:

$$n\lambda = 2d\sin\theta$$
$$a_{GeSn} = 4d$$

Lattice Constants:

a_{GeSn}= 5.679 Å
a_{GeSn}= 5.699 Å
a_{GaAs} = 5.653 Å
a_{Sn}= 6.489 Å
a_{Ge}= 5.658 Å

Vegard's Law:

$$a_{Relaxed}(y) = aSny + aGe(1-y)$$

$a_{||} = a_{substrate}$**= 5.653 Å** *(Pseudomorphic Condition)*

$$a_{\perp} = (1+\varepsilon_{\perp})a_{Relaxed}(y)$$

$$\varepsilon_{\perp} = -\frac{2v}{1-v}\varepsilon_{||}$$ Poisson Ratio: $v = 0.3$

$$\varepsilon_{||} = \frac{a_{||}}{a_{Relaxed}(y)} - 1 \quad < 0$$

~~If layers is fully *relaxed*, the % Sn is 2.6% and 5.0%~~
If layers is fully *strained*, the % Sn is 1.2% and 2.6%

Haley B. Woolf et al., 2022 AVS Symposium, Pittsburgh, PA, USA. November 2023.

Pseudodielectric function before/after cleaning: 1.2%

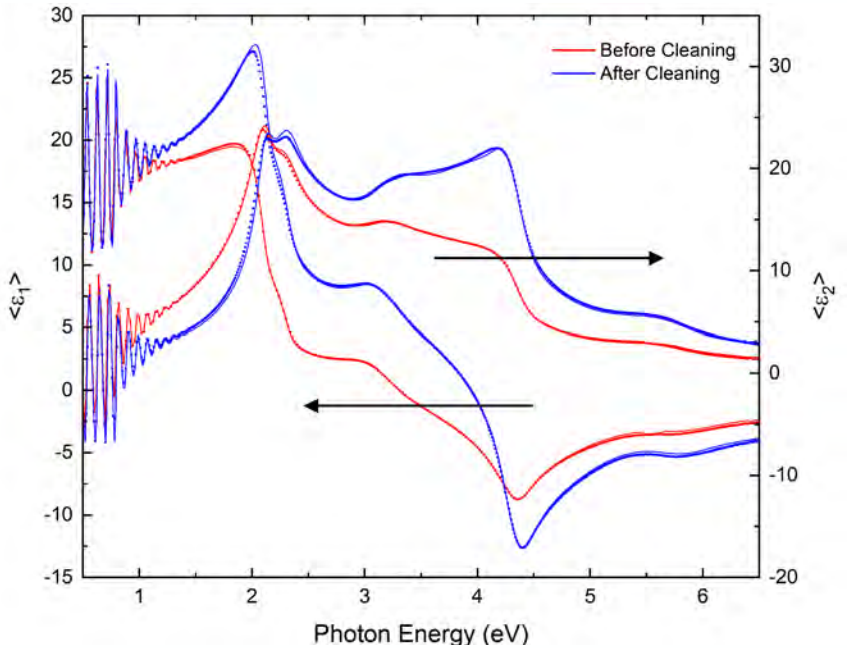

	Oxide Thickness
As Received (May 20th):	43.66 Å
Before Cleaning (June 14th):	72.07 Å
After Cleaning (June 14th):	26.50 Å
After 2nd Cleaning (June 15th):	25.90 Å

The $Ge_{1-y}Sn_y$ on GaAs sample was cleaned ultrasonically with water and then isopropanol for 15 mins each to remove organic layers and most of the native oxide.

Haley B. Woolf et al., 2022 AVS Symposium, Pittsburgh, PA, USA. November 2023.

Pseudodielectric Function

GeSn on GaAs 1.2%

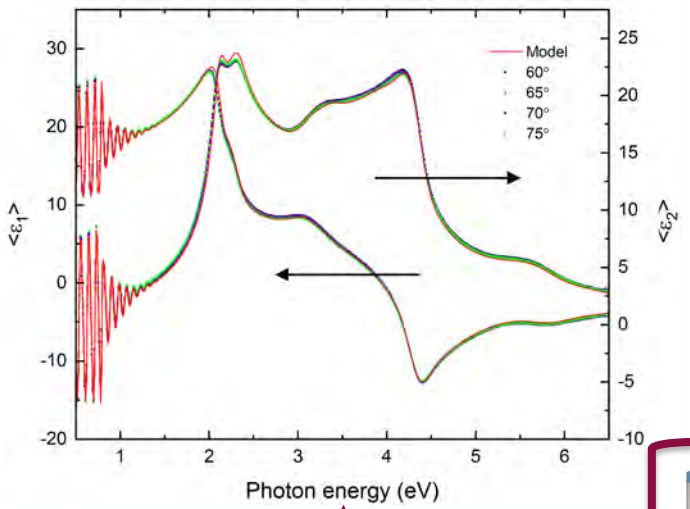

GeSn on GaAs 2.6%

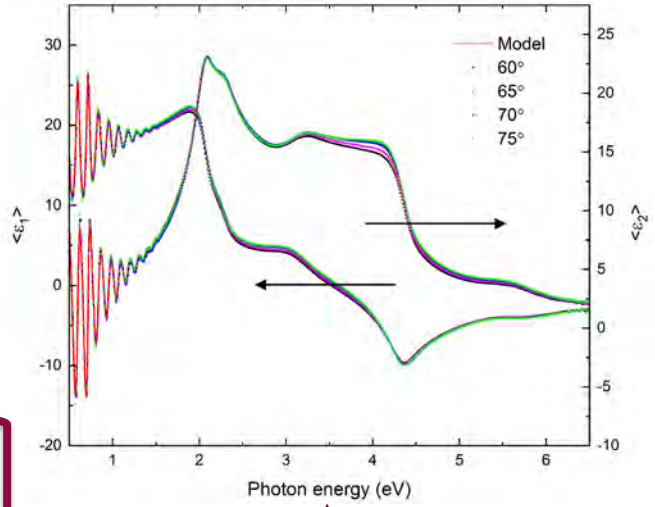

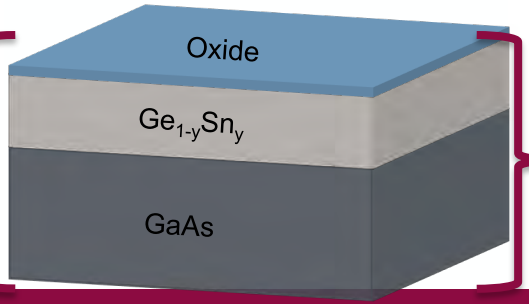

Haley B. Woolf et al., 2022 AVS Symposium, Pittsburgh, PA, USA. November 2023.

$Ge_{1-y}Sn_y$ optical constants

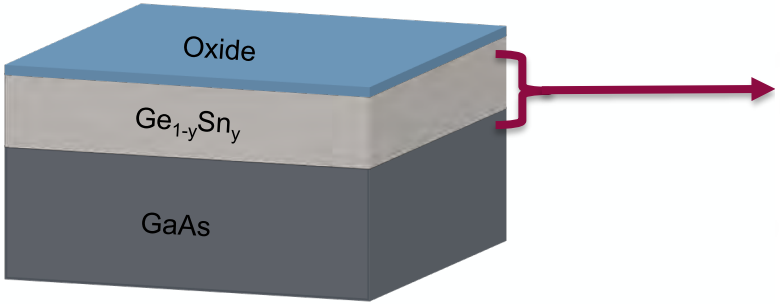

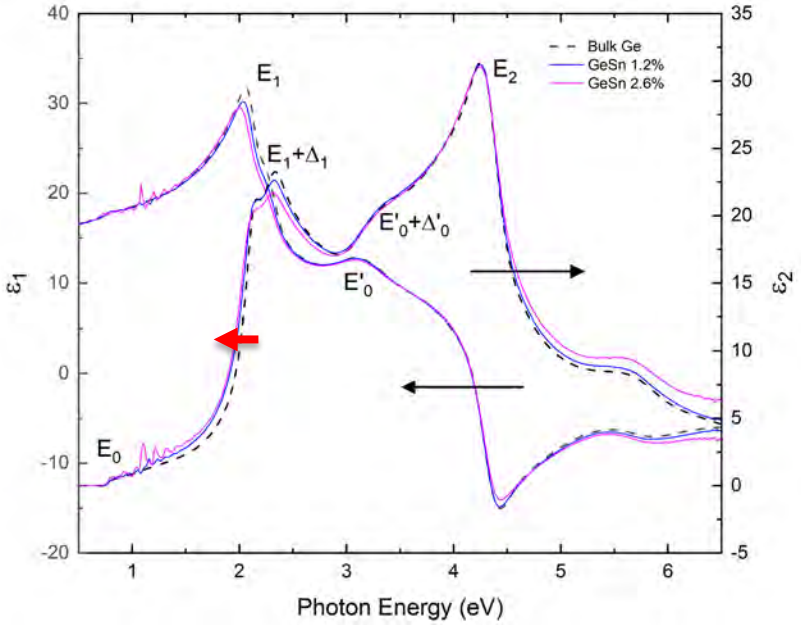

Haley B. Woolf et al., 2022 AVS Symposium, Pittsburgh, PA, USA. November 2023.

2nd Derivative of the dielectric Function: 2.6% tin

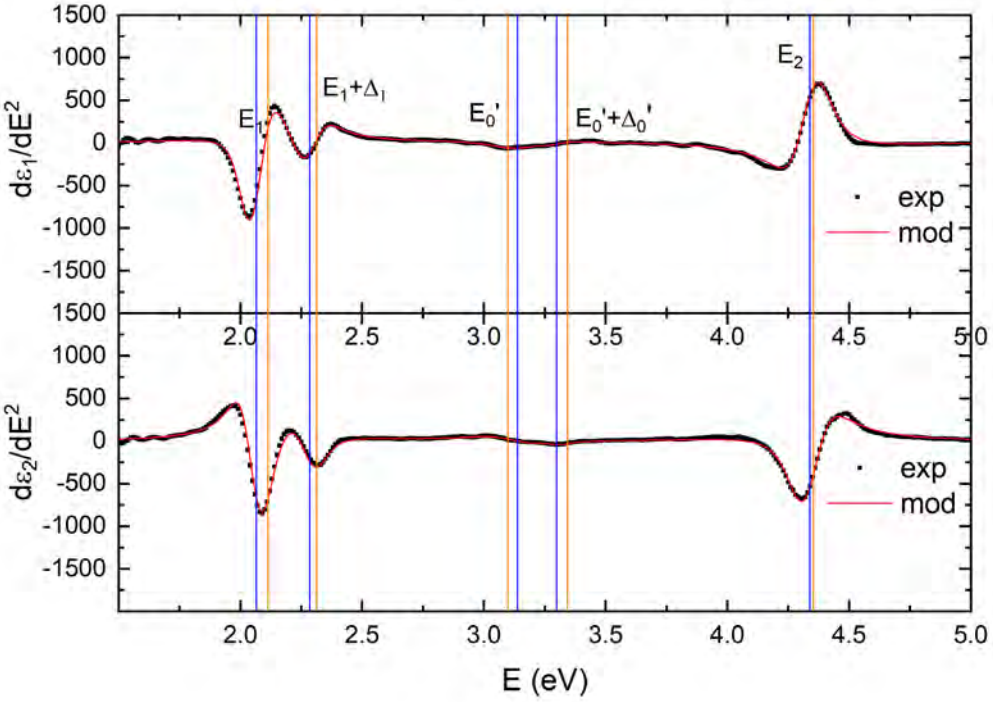

$$\frac{d^2\varepsilon}{d\omega^2} = \frac{Ae^{i\phi}}{(-E_g - i\Gamma + \omega)^2}$$

Critical Points of GeSn 2.6%

CP	E (eV)	A	Φ (deg)	Γ (meV)	n
E_1	2.066	6.701	225.0	0.0769	0
$E_1+\Delta_1$	2.285	2.958	225.0	0.0862	0
E'_0	3.138	2.669	314.9	0.2027	0
$E'_0+\Delta'_0$	3.299	0.060	189.3	0.0485	0
E_2	4.339	10.72	232.9	0.1148	0
CP	E (eV)	A	Φ (deg)	Γ (meV)	n
E_1	2.113	5.32	246	0.050	0
$E_1+\Delta_1$	2.314	3.53	246	0.066	0
E'_0	3.099	1.33	175	0.102	0
$E'_0+\Delta'_0$	3.344	0.486	266	0.139	0
E_2	4.354	11.2	318	0.097	0

Haley B. Woolf et al., 2022 AVS Symposium, Pittsburgh, PA, USA. November 2023.

Dependence of E_1 & $E_1+\Delta_1$ energies on tin content

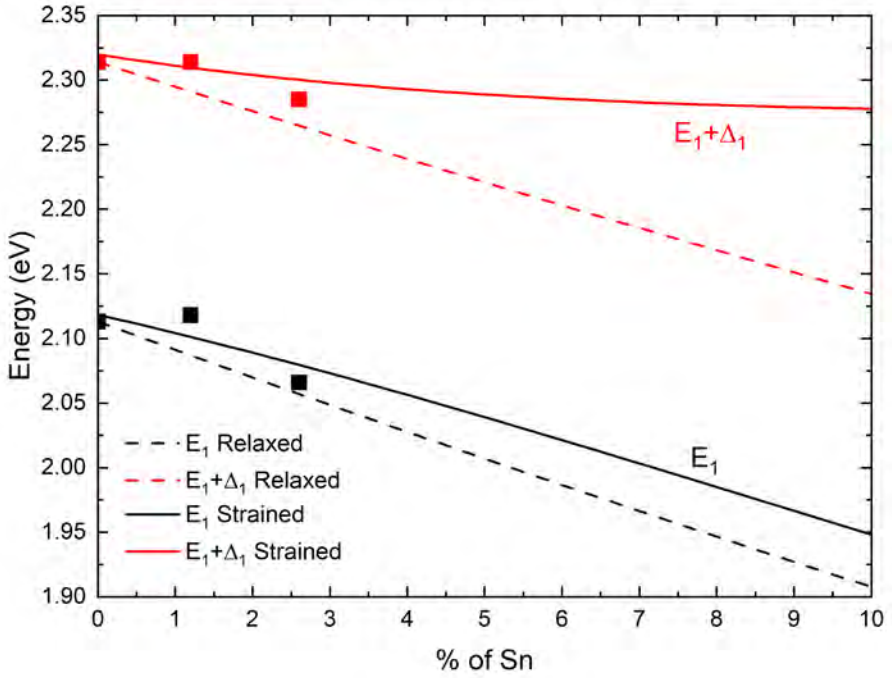

Relaxed:

$$E_1^{GeSn} = yE_1^{Sn} + (1-y)E_1^{Ge} - b_{GeSn}y(1-y)$$

$$(E_1+\Delta_1)^{GeSn} = y(E_1+\Delta_1)^{Sn} + (1-y)(E_1+\Delta_1)^{Ge} - b_{GeSn}y(1-y)$$

$$b_{GeSn} = 1.350 \text{ eV}$$

Strained:

$$E_1^{GeSn} = E_1^{Relaxed} + \Delta E_H - \frac{\Delta E_s^2}{\Delta_1}$$

small shear approximation $\Delta E_s \ll \Delta_1$

$$(E_1+\Delta_1)^{GeSn} = (E_1+\Delta_1)^{Relaxed} + \Delta E_H + \frac{\Delta E_s^2}{\Delta_1}$$

$$\Delta E_H = \sqrt{3}\left[yD_1^{1\,Sn} + (1-y)D_1^{1\,Ge}\right]\varepsilon_H$$

$$D_1^{1\,Sn} = -5.4 \text{ eV}, \quad D_1^{1\,Ge} = -8.7\text{eV}, \quad \varepsilon_H = \frac{\varepsilon_\perp + 2\varepsilon_{||}}{3}$$

$$\Delta E_S = \sqrt{6}\left[yD_3^{3\,Sn} + (1-y)D_3^{3\,Ge}\right]\varepsilon_S$$

$$D_3^{3\,Sn} = -3.8 \text{ eV}, \quad D_3^{3\,Ge} = -5.6 \text{ eV}, \quad \varepsilon_S = \frac{\varepsilon_\perp - \varepsilon_{||}}{3}$$

Photoluminescence spectra of Ge-Sn alloys at 300K

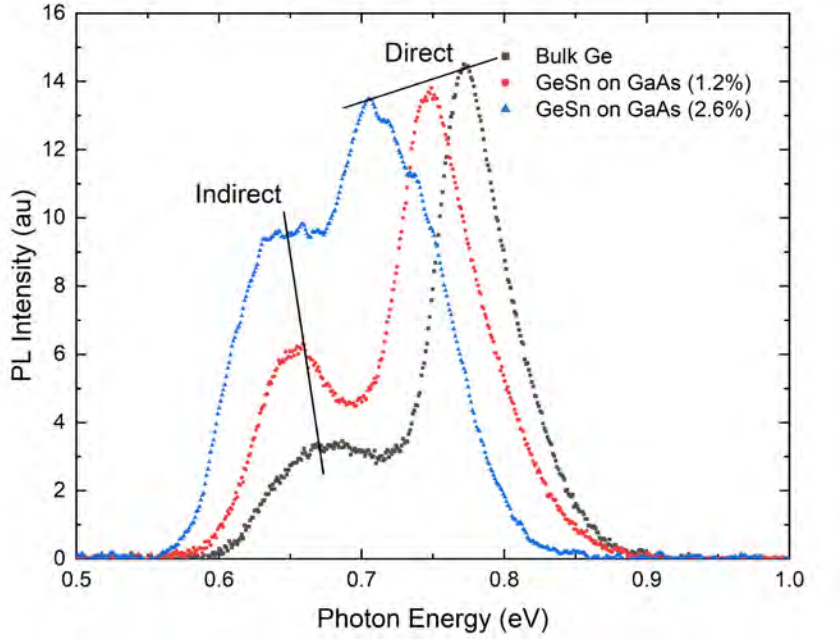

	Indirect Bandgap (eV)	Direct Bandgap (eV)
Bulk Ge:	0.679	0.772
GeSn (1.2%):	0.657	0.748
GeSn (2.6%):	0.651	0.705

Haley B. Woolf et al., 2022 AVS Symposium, Pittsburgh, PA, USA. November 2023.

Dependence of direct bandgap E_0 on tin content

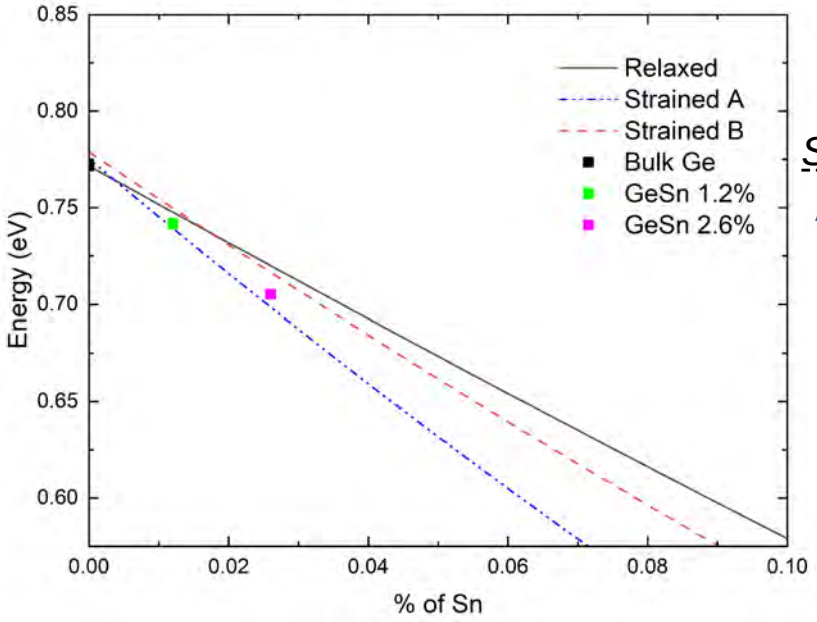

Relaxed:

$$E_0^{GeSn} = yE_0^{Sn} + (1-y)E_0^{Ge} - b_{GeSn}y(1-y)$$

$b_{GeSn} = 2.46$ eV

Strained:

A $$E_0^{GeSn} = E_0^{Relaxed} + \frac{\Delta_0}{2} + \frac{3}{2}b\varepsilon_S + \frac{1}{2}\sqrt{\Delta_0^2 + 6\Delta_0 b\varepsilon_s + (9b\varepsilon_s)^2} + \Delta E_{V2} + \Delta E_C^{\Gamma}$$

B $$E_0^{GeSn} = E_0^{Relaxed} + \Delta E_{V2} + \Delta E_C^{\Gamma}$$

$$\Delta E_c^{\Gamma} = 3[ya^{Sn} + (1-y)a^{Ge}]\varepsilon_H$$

$a^{Sn} = -9.75$ eV, $a^{Ge} = -9.75$ eV, $\varepsilon_H = \frac{\varepsilon_\perp + 2\varepsilon_{||}}{3}$

$$\Delta E_{V2} = 3[yb^{Sn} + (1-y)b^{Ge}]\varepsilon_S$$

$b^{Sn} = -2.3$ eV, $b^{Ge} = -2.3$ eV, $\varepsilon_S = \frac{\varepsilon_\perp - \varepsilon_{||}}{3}$

Haley B. Woolf et al., 2022 AVS Symposium, Pittsburgh, PA, USA. November 2023.

Conclusion

- The (224) reciprocal space maps showed that the GeSn epitaxial layer was grown pseudomorphically on both samples.
- Using Vegard's Law, continuum elasticity theory, and the (004) reciprocal space map, the tin content is found to be y=0.012 and y=0.026.
- After cleaning the sample, the thickness of the oxide was reduced to 26 Å and 23 Å.
- Using the ellipsometry data, the fitted GeSn dielectric function was similar to bulk Ge most likely because of the low tin content.
- The fit second derivative of the dielectric function helped find the critical point parameters and compared to bulk Ge.

Conclusions

- Hooke's Law
- Stress and strain tensors
- Elasticity and compliance tensors
- Examples of stress along one, two, and three directions
- Strain measurements using high-resolution x-ray diffraction
- Impact of strain on phonon energies (Raman spectra)
- Impact of strain on band energies with CMOS applications
- Impact of strain on optical spectra of semiconductors
- Example: Germanium-tin alloys grown pseudomorphically on GaAs

Thank you!

Questions?

New slide